P6.1 INVESTIGATING PRECONVECTIVE SYNOPTIC AND FRONTAL HEAVY RAINFALL ATMOSPHERIC SETTINGS UTILIZING PROXIMITY SOUNDINGS

Michael J. Paddock*
NOAA / National Weather Service, Phoenix, Arizona

Charles E. Graves
Saint Louis University, St. Louis, Missouri

Jason T. Martinelli
Creighton University, Omaha, Nebraska

1. INTRODUCTION

Extreme rainfall is just one type of treacherous weather event, but it has an enormous impact on all facets of transportation (WIST 2005). Two important societal impacts that arise from heavy rainfall include loss of visibility and flash flooding. As visibility decreases, the speed of traffic must also decrease to avoid accidents, especially when traffic flow is increasing (e.g., during local rush hours; WIST 2002). This is true for all modes of transportation. Flash flooding, just as with a loss of visibility, occurs quickly on small time scales and is potentially deadly. According to the National Oceanic and Atmospheric Administration (NOAA 2006), every year flooding costs an average of over 2 billion USD in damages and causes over 100 fatalities. In recent years the flash flood threat has risen due to increasing urbanization. As areas become more populated and are covered with impermeable structures and surfaces such as buildings and roads, the amount of storm-water runoff increases (Kelsch 2002). Consequently, modest rainfall episodes can become potentially dangerous flash flood situations.

Therefore, increased accuracy of forecasting the location and amount of precipitation is crucial in not only saving lives but also reducing property damage. However, quantitative precipitation forecasts (QPF) still lack the precision and confidence shown in other forecast products and remains one of the most difficult tasks in operational meteorology (Junker 2001). According to the United States Weather Research Program (USWRP 2001) and the National Weather Service (NWS), one of the top priorities is to increase the accuracy of QPF.

* *Corresponding author address:* Dr. Michael J. Paddock, NOAA / National Weather Service, Phoenix, AZ.
Email: Michael.Paddock@noaa.gov

According to WIST (2002), the highway carrying capacity is expected to multiply, which will multiply the economic and safety impacts due to adverse weather and weather-related road conditions. These societal and economic concerns, associated with even moderate rainfall, make the operational forecasting of these events paramount.

1.1 OBJECTIVE

This work is an attempt to apply several proximity-sounding techniques from previous researchers toward a different atmospheric phenomenon, heavy rainfall. To accomplish this, observational and Rapid Update Cycle Version II (RUC-2) analysis soundings were collected in the preconvective environments of heavy rainfall producing storms (rainfall event selection is illustrated in Section 3). Numerous sounding parameters were investigated to distinguish environmental differences between rainfall amounts (greater than or equal to four inches versus two inch rainfall days). This type of study has been conducted for severe weather events (e.g., tornadoes), but not for a large heavy rainfall dataset.

2. RELATED LITERATURE

2.1 OBSERVATIONAL SOUNDINGS

Darkow (1969), Houze et al. (1990), Brooks et al. (1994), and Rasmussen and Blanchard (1998) have studied the advantages of proximity soundings, using observational soundings, associated with warm season severe weather. Many obstacles present themselves when considering observational proximity soundings.

First, there are questions regarding the most relevant location for a severe weather proximity sounding. Second, severe weather such as supercells are essentially randomly distributed with respect to the observational soundings, making consistent data collection difficult at best.

Beebe (1955) discovered soundings taken in a very close time and space proximity to tornadoes had noticeably different vertical structures compared to proximity soundings in the antecedent pre-convective environment several hours earlier. Supercells may exert influence on low-level shear and buoyancy profiles up to 30 km away from the storm, effectively altering what had been the pre-storm environment (Weisman et al. 1998). This illustrates that the proximity sounding should be chosen relatively close to the event, temporally and spatially. There are other concerns a researcher will most likely be presented with, such as sounding sample size and storm characteristics for their particular situations. The studies of Brooks et al. (1994) and Rasmussen and Blanchard (1998) illustrated that observational soundings are quite capable of serving as proximity soundings even when adjusting certain spatial and temporal allowances to increase the size of a dataset. Brooks et al (1994) discovered that a spatial distance of 160 km and a temporal allowance of ±1 hour from the nominal sounding time allowed for more cases without harming the quality of the dataset. Rasmussen and Blanchard (1998) defined their proximity soundings as inflow sector soundings based on the boundary layer mean wind vector. The sounding was assumed to be in the inflow sector of any meteorological event if it was within 400 km and the event fell within a 150° sector centered on the boundary layer mean wind vector.

2.1 MODEL ANAYLYSIS SOUNDINGS

A primary advantage to the use of model analysis grids is the collection of a much larger sample of storm cases in a shorter period of time. For example, RUC-2 model analyses contain asynoptic data from wind profilers, aircraft temperatures and winds, satellite-derived winds, surface observing networks, etc. However, model analysis grids must be consistent with observed data if they are to serve as a diagnostic tool, and the analysis grids must be available frequently, from a temporal perspective, so that changes in parameters can be observed over a mesoscale temporal domain (Thompson and Edwards 2000). Thompson et al. (2003), Edwards and Thompson (2000), and Thompson and Edwards (2000) investigated RUC-2 model soundings as effective proximity soundings. Thompson and Edwards (2000) chose the nearest (i.e., to the supercell) available RUC-2 grid point data in the inflow sector of the supercell. They also normalized the RUC-2 soundings to the equilibrium level (EL) height by dividing each sounding into ten equal height layers from the surface to the EL. This allowed them to relate various types of supercell storms (e.g., light precipitation, heavy precipitation, classic, and mini-supercells) to one another based upon sounding-derived parameters within the ten equal height layers.

The results Thompson and Edwards (2000) found are critical and therefore must be explained in some detail to completely understand the biases of the RUC-2 model. The RUC-2 analysis soundings were found to be characteristically 1 to 2°C too dry at the surface and 850 hPa, as well as 1 to 2°C too cool at the surface and too warm at 850 hPa, when compared to observed soundings at the same time and location. This minor cool and dry bias of the RUC-2 soundings at the surface, combined with the warm bias at 850 hPa, contributed to a tendency for convective inhibition to be somewhat overestimated, and surface-based CAPE to be underestimated by approximately 500-1000 Jkg^{-1}. Temperature errors in the middle and upper troposphere were substantially smaller than in the lower troposphere, therefore, the CAPE errors were basically the result of a cool and dry surface bias of the RUC-2 analyses. They discovered the potential for some of the surface errors to be the result of differences between the RUC-2 surface pressures and those of the co-located observations, as well as due to the interpolation differences in the RUC-2 soundings constructed from grids of 25 hPa vertical resolution.

As with surface temperatures and low-level dew points, Thompson and Edwards (2000) discovered that the majority of the vertical shear parameters were slightly underestimated in the RUC-2 analysis soundings. Parameters such as 0-3 km system-relative helicity (SRH) and the bulk Richardson number (BRN) shear term, which incorporate low-level details from the hodograph, were most sensitive to small variations in the compared wind profiles. The mean absolute analysis errors for the BRN shear term and 0-3 km SRH were substantial, though small negative mean errors suggested only a slight tendency for the RUC-2 analysis hodographs to consistently underestimate low-level vertical shear. The 0-6 km wind vector difference showed even less variation between the observations and RUC-2 analyses. The errors in the RUC-2 model soundings, when compared to observational soundings at the same time and location, were found to be within instrumentation measurement errors (Thompson and Edwards 2000). Therefore, even given the errors of the model, unmodified RUC-2 model

analysis soundings may be utilized as proximity soundings.

3. DATA AND METHODOLOGY

The General Meteorological Package (GEMPAK; Koch et al. 1983), software and Saint Louis University's SLUbrew diagnostic analysis program were used to diagnose and display key parameters on surface and upper-air plots. Also, both sets of software use the Barnes (1973) objective analysis to objectively analyze the data being examined. To statistically analyze the significant difference between sounding parameters for each atmospheric setting, the Statistical Package for the Social Sciences (SPSS) was used.

In GEMPAK, observational data as well as 3-hourly RUC-2 (Benjamin et al. 2004) initialization model data, acquired from the NWS observational network via Unidata's Internet Data Distribution (IDD) network, were used in the analysis of the synoptic setting, moisture, instability, and wind shear parameters. For the four and two inch rainfall cases in this study, GEMPAK surface analyses were created to diagnose the location of the extratropical cyclones (ETC) and their associated fronts and precipitation. The surface station plots were created from surface METAR observations using GEMPAK. Upper-air station plots and analyses were created from the NWS operational upper-air observations using GEMPAK. These plots were generated to help classify these rainfall events into various Maddox et al. (1979) atmospheric settings. The sounding parameters were then divided into the various atmospheric settings, where a statistical analysis (described below) was conducted between each Maddox et al. (1979) setting and between each rainfall category. Of interest, in this study, is the statistical analysis between rainfall categories based on specific atmospheric settings.

SLUbrew, created by Graves and Moore (2002), uses upper-air and surface data, from the NWS via IDD, to diagnose various basic and derived parameters. Upper-air data is collected twice daily (0000 UTC and 1200 UTC) for over 100 stations, spaced approximately 400 km apart, across North America. These data are archived at Saint Louis University in the form of soundings containing temperature, dewpoint, wind direction and speed information for all mandatory and significant pressure levels. Surface data are collected from over 600 observation stations for every hour. These datasets are also archived at Saint Louis University in METAR form, and contain temperature, sea level pressure, cloud cover, precipitation type and intensity, wind direction and speed, and hourly barometric tendency. Daily rainfall accumulation plots were used to show the location(s) of the greatest rainfall accumulation. These data were obtained through the National Climatic Data Center (NCDC) River Forecast Center (RFC). Doppler radar (WSR-88D) data, obtained from NCDC and the University Corporation for Atmospheric Research (UCAR), were used to determine the location, orientation, intensity, and movement of the precipitation field with units given in decibels (dBz).

SPSS is a statistical package, which analyzed the data from various parameters for all soundings within the datasets. This included checking for statistically significant differences between four and two inch rainfall sounding parameters. Of greater interest, this software was used to compare four and two inch rainfall sounding parameters within their respective atmospheric settings (i.e., synoptic, frontal, mesohigh) to determine which parameters, if any, would best distinguish between four and two inch rainfall days given a specific Maddox et al. (1979) atmospheric setting.

3.1 DETERMINING SIGNIFICANT DIFFERENCES

In order to determine whether a parameter or multiple parameters are significantly different from one rainfall category to the next, two statistical evaluations were conducted. The first statistical procedure was to generate boxplots (i.e., box-and-whisker plots). The second statistical procedure utilized the Mann-Whitney test statistic to determine whether the means of each distribution are significantly different between the rainfall categories.

Boxplots are a frequently used graphical tool that depicts five simple statistics. The minimum, lower quartile (25th percentile), median (50th percentile), upper quartile (75th percentile), and the maximum values are illustrated in boxplots. These five statistics, within the boxplot graphic, allow an individual to quickly examine the distribution of the data (Wilks 2006). When boxplots of a particular parameter for all rainfall categories are aligned side-by-side it shows how that particular parameter may vary from one rainfall category to the next. If the "box" portion of the boxplots overlaps from one category to the next, then there is potentially no statistically significant difference between the rainfall categories for that particular parameter. However, if the "box" portions do not overlap, then there is a

higher probability of a significant difference between the rainfall categories. To help discern these differences, the Mann-Whitney test statistic is utilized.

While boxplots are extremely helpful and give a quick representation of the distribution, they lack additional insight. The Mann-Whitney test statistic gives further detail of the data in question. The Mann-Whitney test is a nonparametric test for location (i.e., difference between the means) for two independent (i.e., both serially independent, and unpaired) samples. It is extremely useful as it does not require the user to assume a distribution (Wilks 2006). When the boxplots indicate an increase or decrease (i.e., a difference) in parameter values from one category to the next, but the "box" portions still overlap, the Mann-Whitney test was used to determine if there is a statistically significant difference between the categories even though the boxplots do not indicate this statistical difference. The combination of the boxplots and the Mann-Whitney test were used to determine which parameters illustrate a significant difference between rainfall categories. These significant parameters are utilized to best discern a difference between rainfall accumulations associated with different atmospheric settings.

Once the three-year (2003-2005) statistical dataset was generated, it was further examined by comparing those results to those of individual precipitation events that occurred in the years 2006-2007. This determined which, if any, parameters illustrated a consistent statistical trend in not only the larger dataset comparison, but also when investigating individual cases. These individual events from 2006 through 2007 are representative of what forecasters would be challenged with in a day-to-day operational setting. These heavy precipitation parameters, that illustrate this consistent, statistical trend, in the three-year dataset and individual event comparison, will allow forecasters to determine if there is a potential for a significant heavy rainfall episode for their area.

3.2 CASE SELECTION

Parameters and processes are examined using the software described in Section 3 for 33 case studies associated with rainfall accumulations equal to or greater than four inches from 2003-2005 (4 cases from 2006-2007) and 47 case studies associated with rainfall accumulations between one and two inches from 2003-2005 (4 cases from 2006-2007). The four inch or greater heavy rainfall cases were chosen on the following basis:

- Rainfall events occurred during the warm season (March through September) in the central United States for the years 2003 through 2007.
- Storm Data publication listed an event under the categories of heavy rainfall, flooding, and/or flash flooding.
- The Climate Prediction Center River Forecast Center 24-hour rainfall accumulation plots indicated rainfall accumulations greater than or equal to four inches with reports from more than one station. These plots were also compared to the Storm Data listing of an event for cross-referencing.
- Doppler radar depicted the rainfall was generated from one precipitation system and not waves of precipitation. It is also used to determine the timing of the precipitation near observational sounding sites.
- Observed soundings were collected if they occurred within six hours prior to and 250 km of the event.
- Model analysis soundings were collected in close temporal and spatial proximity to an event.

The one and two inch light rainfall cases were chosen on the following basis:

- Rainfall events occurred during the warm season (March through September) in the central United States for the years 2003 through 2007.
- The Climate Prediction Center River Forecast Center 24-hour rainfall accumulation plots indicated rainfall accumulations between one and two inches with reports from more than one station.
- Doppler radar depicted the rainfall was generated from one precipitation system and not waves of precipitation. It is also used to determine the timing of the precipitation near observational sounding sites.
- Observed soundings were collected if they occurred within six hours prior to and 250 km of the event.
- Model analysis soundings were collected in close temporal and spatial proximity to an event.

After dividing the four-inch and two-inch datasets into various atmospheric settings, the results from comparing the four-inch dataset with the two-inch dataset and all the statistical analyses of the numerous parameters, associated with each comparison, are illustrated in Section 4. Section 5 provides a summarization of the results.

4. RESULTS

4.1 SYNOPTIC-TYPE EVENTS

The comparison between four-inch and two-inch rainfall days associated with a synoptic-type heavy rainfall setting illustrated numerous parameters that showed significant variations between rainfall categories. These variations in moisture, instability, wind shear, and other parameters are discussed within this section.

When investigating key moisture parameters, each parameter showed an increase (i.e., an increase in atmospheric moisture) from the two-inch category to the four-inch category. These key parameters are K index, precipitable water (PW), subcloud layer relative humidity, surface-500 hPa relative humidity, and surface-500 hPa theta-e. An increase in these values was anticipated since there is an increase in rainfall amount. The boxplots of these moisture parameters illustrate the increasing values from the two-inch to four-inch rainfall category. Illustrated in Figure 1 are the K index values. Figure 2 depicts the increase in PW values. Others parameters (not shown) follow the same pattern. However, the “box” portions of the boxplots still overlap, and therefore, potentially, do not depict a significant difference between rainfall categories. Thus, the Mann-Whitney test statistic was generated to determine if the means from the two rainfall distributions were significantly different. All moisture parameters demonstrated a less than one percent chance that the two rainfall distributions are related, or could have come from the same population. Thus, they are significantly different.

The 850-500 hPa convective instability (Fig. 3) and lid strength index (not shown) values decrease from the two-inch to four-inch rainfall categories. Coinciding with this decrease in stability, most unstable parcel convective available potential energy (MUCAPE; Fig. 4) increases across the rainfall categories. It is evident that the atmosphere is less stable for the four-inch rainfall days when compared to the two-inch days.

The boxplots, for the instability parameters, show similar results as the moisture parameters, therefore, the Mann-Whitney test was utilized once again. Nearly all instability parameters illustrated a less than one percent chance of the two rainfall categories arising from the same population. Two parameters, most unstable parcel convective inhibition and convective temperature, demonstrated higher percentages, 2.385 and 20.327 respectively, illustrating that, at least, convective temperature is not as crucial as other parameters, when determining rainfall accumulation potential.

Bulk wind shear (speed and directional) parameters were investigated to decipher the potential impact of wind shear on the local environments associated with these rainfall events. 0-2, 0-3, 0-6, and 3-6 km speed and directional bulk shear were compared. Looking for differences between the boxplots (i.e., distributions), only two parameters depicted a difference. 0-3 km (Fig. 5) and 3-6 km (Fig. 6) speed shear illustrate a decrease (i.e., a decrease in wind speed) from the two-inch to four-inch rainfall category. When compiling the Mann-Whitney statistic for these two parameters, only the 3-6 km speed shear demonstrated a less than one percent chance that the two categories could be from the same population. The 0-3 km speed shear showed a greater than 20% chance the two rainfall categories are related. Less wind speed shear at the 3-6 km range, for the four-inch rainfall events, illustrates a weaker steering mechanism and, therefore, weaker storm-cell advection. This allows more precipitation to accumulate in a shorter period of time over a particular region.

Additional parameters investigated include the equilibrium temperature, the distance between the level of free convection (LFC) and the equilibrium level (EL), the pressure level of the LFC, the pressure level of the lifted condensation level (LCP), and the warm cloud depth. All of which use the most unstable parcel, except the LCP. The equilibrium temperatures (Fig. 7) show colder temperatures for the four-inch rainfall category than the two-inch. Also, the distance between the LFC and EL (Fig. 8) increases from the two-inch to four-inch rainfall category. The last two parameters that appeared interesting are the LCP (Fig. 9) and warm cloud depth (Fig. 10). LCP values increased (i.e., lower LCL heights), while the warm cloud depth values also increased, which makes sense with lower LCL and LFC heights, but also indicates slightly higher freezing levels in the atmosphere. The Mann-Whitney statistics identified the top three parameters in this category to be the warm cloud depth, distance between the LFC and EL, and the LCP with percentages of 0.013, 0.357, and 1.578, respectively. Once again, this test statistic

illustrates a strong difference between the two rainfall categories.

These last few parameters combined with several instability and moisture parameters illustrate a different four-inch sounding profile than the two-inch profile. With lower LCL heights, colder equilibrium temperatures, a greater distance between the LFC and EL, and an increase in MUCAPE values indicates a longer (taller), moister, and less stable profile than the two-inch rainfall events. Also, the increase in warm cloud depth values illustrates that heavier rainfall events rely on warm cloud precipitation processes to produce greater rainfall accumulations.

4.2 FRONTAL-TYPE EVENTS

The comparison between four-inch and two-inch rainfall days associated with a frontal-type heavy rainfall setting illustrated some surprising results. Numerous parameters that showed significant variations in the synoptic-type setting did not show the same results here. When investigating key moisture parameters, only three parameters showed an increase (i.e., an increase in moisture) from the two-inch category to the four-inch category. These key parameters are PW, subcloud layer relative humidity, and surface-500 hPa relative humidity. Once again, an increase in these values was expected since there is an increase in rainfall amount, but for only three parameters to show a difference between rainfall categories was surprising. The boxplots of these parameters illustrate the increasing values. Illustrated in Figures 11, 12, and 13 are PW, subcloud layer relative humidity, and surface-500 hPa relative humidity, respectively. The boxplot values for the K index are shown in Figure 14 to illustrate a lack of separation between the two rainfall categories. Looking at the K index median values for each rainfall category, they are equal (32) demonstrating that the values in both distributions are distributed nearly equally. Others parameters (not shown) follow the same pattern as the K index values.

The Mann-Whitney test statistic was generated to determine if the means from the two rainfall distributions were significantly different for the three parameters that indicated a difference (i.e., an increase in moisture). Of the three moisture parameters, only one demonstrated a less than one percent chance that the two rainfall distributions are related, or could have come from the same population. This parameter was the surface-500 hPa relative humidity with a percentage of 0.038. The other two, PW and subcloud layer relative humidity, have percentages of 12.714 and 3.438, respectively.

The 700-500 hPa lapse rates (Fig. 15), 850-500 hPa convective instability (Fig. 16), and convective temperature (not shown) illustrate differences from the two-inch to four-inch rainfall categories. These are the only instability parameters that depict a difference between rainfall categories. This was a surprise as well. The Mann-Whitney test was utilized once again. Of the three instability parameters that showed a difference, utilizing boxplots, only one illustrated a less than one percent chance that the two rainfall categories could be from the same population. 700-500 hPa lapse rates have a percentage of 0.199. The other two parameters (850-500 hPa convective instability and convective temperature) have demonstrated higher percentages that just happen to be identical (10.383%). Therefore, it is not as evident as the synoptic-type heavy rainfall events that the atmosphere is less stable for the four-inch rainfall days when compared to the two-inch days. It appears that the instability of the atmosphere is nearly identical for both rainfall categories. What is interesting is that the 700-500 hPa lapse rates illustrate that the two-inch events have steeper mid-level lapse rates, which increases CAPE. In this way, the two-inch events need steeper lapse rates to achieve greater instability whereas the four-inch events do not. This was also noticed in the synoptic-type events.

Just as with the synoptic-type heavy rainfall events, bulk wind shear (speed and directional) parameters were investigated. Looking for differences between the boxplots (i.e., distributions), only one parameter depicted a difference, 3-6 km directional shear (not shown), illustrates a change in wind direction from a northerly to a northwesterly direction from the two-inch to four-inch rainfall category. Otherwise, just as with the instability parameters, the atmospheres associated with the two rainfall categories are very similar with respect to no significant differences in wind shear.

Additional parameters investigated also show little change between rainfall categories. These, once again, include the equilibrium temperature, the distance between the LFC and the EL, the pressure level of the LFC, LCP, and the warm cloud depth. Of these parameters, only three showed slight differences between rainfall categories. The distance between the LFC and EL (Fig. 17), LCP (Fig. 18), and the pressure level of the LFC (Fig. 19) depict an increase in values from the two-inch to four-inch categories. Therefore, there are lower LFC and LCL heights in the four-

inch rainfall category than the two-inch, which allows for the greater distance between the LFC and EL. The Mann-Whitney statistics depicted the top three parameters in this category to be the distance between the LFC and EL, LCP, and the pressure level of the LFC with percentages of 4.363, 4.846, and 7.353, respectively. Once again, given these percentages, this does not illustrate a tremendous difference between the two rainfall categories when compared to other moisture and instability parameters, but it does indicate a 95% confidence that the two rainfall categories are different with respect to the distance between the LFC to the EL and the LCP.

These last few parameters combined with instability, moisture, and wind shear parameters illustrate that there are minor differences between the four-inch sounding profile than the two-inch profile. Only two parameters illustrating a less than one percent chance that the two rainfall categories could be from the same population; and another four parameters illustrated a less than five percent chance. It becomes evident that a forecaster will have a more difficult time discerning whether a frontal-type heavy rainfall event will produce rainfall accumulations of two inches or greater than four inches just by utilizing proximity soundings. Perhaps strength and overall movement of the system should be considered.

4.2 DATASET FORECAST VERIFICATION

To examine the potential forecast strength of the statistical dataset from the years 2003-2005, it is essential that the heavy rainfall parameters, that illustrated a statistical difference between rainfall categories, be compared to individual cases from the years 2006-2007, similar to what forecasters would face in an operational setting. To accomplish this, individual cases were chosen utilizing the same criteria as the three-year dataset. Parameters were generated from proximity soundings and compared to those from the three-year dataset for their specific atmospheric setting and rainfall accumulation category.

When investigating the parameters and statistics (shown in Tables 1 through 4) associated with these new, test case datasets, they appear to fit each rainfall and atmospheric setting category, from the original, three-year dataset (parameters and statistics shown in Tables 5 through 8), quite well. The parameter values associated with these test cases fall within the full range of values associated with the original, three-year rainfall categorical datasets. Therefore, these new events will be a great addition to the original dataset, There are, however, some differences that are worth noting when comparing rainfall categories from the test case dataset to that of the original, three-year dataset. It appears that K index and PW are the two parameters that illustrated noticeable differences in the comparison. There does not seem to be a particular threshold for either parameter associated with any of the rainfall categories or atmospheric settings. For example, there tends to be a range of K index and PW values that overlap when comparing rainfall categories for the various atmospheric settings. Thus, on a case-by-case basis, K index and PW appear not to be the best discriminating parameters. These are differences that help to illustrate that, in a case-by-case situation, some parameters that demonstrate a difference between rainfall categories, when utilizing large statistical datasets, do not always apply to individual events.

As just stated, there are differences between parameters associated with the test cases and those of the larger dataset that would not allow a forecaster to determine if the forecast area has the potential for a heavy rainfall day (greater than four inches) or not. The most notable are K index and PW, which are typically used by forecasters on a daily basis. However, there are several parameters that now seem to stand out from the others. They are the surface-500 hPa relative humidity, subcloud layer relative humidity, LCP, pressure level of the LFC, the distance between the LFC to EL, and the warm cloud depth. While several of these are related (example will follow), they still illustrate a distinction between the rainfall categories for each atmospheric setting. How are some of these parameters related? If the LFC and LCL are lower in the atmosphere, the distance between the LFC and EL is potentially greater (as long as the EL remains at the same height) and the warm cloud depth will be greater as well. Not to mention, with an increase in the distance between the LFC and EL, there will be an increase in CAPE.

It has been mentioned in numerous studies that precipitation efficiency is critical in maintaining a convective system for the greatest rainfall accumulation. Two big sources of reduced efficiency are entrainment of dry air into the convective cell and precipitation evaporation below the cloud base. As shown with statistics, the heavier rainfall events have higher surface-500 hPa relative humidity values, which reduce the amount of dry air entraining into the system, and higher subcloud layer relative humidity values, which reduce the amount of precipitation

evaporation below the cloud base. Also, the added moisture content, below cloud base, allows for a moister updraft, which increases moisture convergence and condensation at low levels. These two critical moisture parameters have shown to be very important in maintaining precipitation efficiency.

When combining the results from the individual parameter comparisons, from the three-year dataset, and the parameters associated with the test cases, several parameters presented themselves with a higher potential for depicting the difference between rainfall categories. When the subcloud layer relative humidity and surface-500 hPa relative humidity are comparatively high, the four-inch rainfall potential is greater than the possibility of a two-inch rainfall day. Also, the CAPE, warm cloud depth, and the distance between the LFC and EL are relatively greater for four-inch rainfall days than two-inch days. Keep in mind that the distance between the LFC and EL increases for four-inch rainfall days, in part, due to the lower LFC and LCP heights. Therefore, in an attempt to quantify these parameters, the subcloud layer relative humidity and surface-500 hPa relative humidity values were multiplied together, scaled, and plotted against the distance between the LFC and EL values. The product of the relative humidity parameters was scaled to eliminate large values. This was conducted for both the four-inch and two-inch rainfall categories and combined into one graph for each atmospheric setting. For the synoptic-type setting, the scatterplot results are illustrated in Figure 20. For the frontal-type setting, the scatterplot results are illustrated in Figure 21.

The majority of the synoptic-type four-inch rainfall events cluster in a particular region, fairly high on the graph, illustrating forecast strength. However, there are several two-inch rainfall events located in this region as well. To help discern a difference between the two precipitation categories, a linear trend was generated and plotted on the same graph. This line depicts the greatest separation between the two rainfall categories. Events that fall above this line have a greater probability of being a four-inch type event. If the event falls below the line, there is a greater probability that the event will be a two-inch type event. Utilizing this linear trend captures nearly 70% of the four-inch events, while limiting the two-inch events by only capturing 35% of them above the line. Another nice feature is that the slope of the trend line is negative, which makes sense. This illustrates that the higher the atmospheric moisture content, the more likely it would be to observe four-inch rainfall events rather than two-inch events. The distance between the LFC and El becomes slightly more negligible as the atmospheric moisture content increases.

Similar results were found with the frontal-type rainfall setting. There is a clustering of four-inch rainfall events in a particular region, relatively high on the graph, but there are a few more four-inch events that are located in the lower portion of the graph than noticed in the synoptic-type events. These might be low-echo centroid convective storms (i.e., small LFC-EL distance with relatively high relative humidity), but more research will need to be conducted to verify this hypothesis. Utilizing the same linear trend concept as before, this also captures nearly 70% of the four-inch events, but also captures 41% of the two-inch events above the line. While this is not bad, it certainly demonstrates that it would be slightly more difficult to forecast a rainfall amount associated with a frontal-type setting rather than the synoptic-type setting. Just as with the synoptic-type events, the slope of the trend line is negative.

It must be stated that in either atmospheric setting, the graphs do inform a forecaster that there are preferred combinations (i.e., clustering of events) that would tend to lead a forecaster toward one rainfall category over another. However, in these situations, a forecaster will still need to investigate other external processes (e.g., moisture flux convergence, theta-e advection, system movement, soil moisture content, etc) to help determine rainfall accumulation potential for their particular event. This study is a means to help a forecaster quantify the rainfall potential.

5. SUMMARY

This work is an attempt to apply several proximity-sounding techniques from previous researchers toward a different atmospheric phenomenon, heavy rainfall. Observational and RUC-2 analysis soundings were collected in the preconvective environments of heavy rainfall producing storms. Numerous sounding parameters were investigated to distinguish environmental differences between rainfall accumulations of greater than or equal to four inches versus rainfall days where only two inches had accumulated. Similar studies have been conducted for severe weather events (e.g., tornadoes), but not for a large heavy rainfall dataset.

The results for the synoptic-type heavy rainfall setting demonstrate the typical results the

researchers anticipated. As the rainfall accumulation increases, the moisture parameters indicate an increase in atmospheric moisture and the stability of the atmosphere decreases. There are lower LCL heights, colder equilibrium temperatures, a greater distance between the LFC and EL, and an increase in MUCAPE values, which indicates a longer (taller), more moist, and less stable profile than the two-inch rainfall events. The increase in warm cloud depth values illustrates that heavier rainfall events rely on warm cloud precipitation processes to produce greater rainfall accumulations. While the majority of the bulk wind shear parameters did not depict noticeable differences between the rainfall categories, the 3-6 km speed shear parameter was the only outlier. This potentially indicates that the wind, in this layer, is not as strong in the four-inch cases, and therefore, the heavy rainfall producing cells are not advected as quickly as they are in the two-inch cases.

On the other hand, the comparison between four-inch and two-inch rainfall days associated with a frontal-type heavy rainfall setting illustrated some surprising results. Numerous parameters that showed significant variations in the synoptic-type setting did not show the same results here. Overall, the moisture, instability, bulk wind shear, and additional parameters illustrate that there are minor differences between the four-inch sounding profile than the two-inch profile. With only two parameters (700-500 hPa lapse rates and surface-500 hPa relative humidity) illustrating a less than one percent chance that the two rainfall categories could be from the same population. Also, only four additional parameters illustrated a less than five percent chance that the two rainfall categories are related.

To examine the potential forecast strength of the statistical dataset from the years 2003-2005, it is essential that the heavy rainfall parameters be compared to individual cases. Individual cases, for the years 2006-2007, were chosen utilizing the same criteria as the original, three-year dataset. Parameters were generated from proximity soundings and compared to those from the three-year dataset for their specific atmospheric setting and rainfall accumulation category. On a case-by-case basis, K index and PW appear not to be the best discriminating parameters. However, there are several parameters that do seem to stand out, statistically, from the others. These parameters are the surface-500 hPa relative humidity, subcloud layer relative humidity, LCP, pressure level of the LFC, the distance between the LFC and EL, and the warm cloud depth. While several of these parameters are linked to one another, they still illustrate a distinction between rainfall categories for each atmospheric setting. Surface-500 hPa relative humidity and subcloud layer relative humidity are two critical parameters that have shown to be very important in maintaining precipitation efficiency.

In an attempt to quantify these distinctive parameters, the subcloud layer relative humidity and surface-500 hPa relative humidity values were multiplied together, scaled, and plotted against the distance between the LFC and EL values. Then, utilizing a linear trend, which best distinguishes between the two rainfall categories, for the synoptic-type setting, results in capturing nearly 70% of the four-inch events, while limiting the two-inch events by only capturing 35% in the same region. Similar results were found with the frontal-type rainfall setting. Utilizing the same linear trend concept as before, this also captures nearly 70% of the four-inch events, while limiting the two-inch events by capturing 41%. These two graphs inform a forecaster that there are preferred combinations (i.e., clustering of events) that would tend to lead a forecaster toward one rainfall category over another. However, in these situations, a forecaster will still need to investigate other external processes to help determine rainfall accumulation potential.

REFERENCES

Barnes, S. L., 1973: Mesoscale objective analysis using weighted time-series observations. Tech. Rep. ERL NSSL-62, NOAA, National Severe Storms Laboratory, Norman, OK 73069, 60 p. [NTIS Com-73-10781].

Beebe, R. G., 1955: Types of air masses in which tornadoes occur. Bull. Amer. Meteor. Soc., 36, 349–350.

Benjamin, S. G., G. A. Grell, J. M. Brown, T. G. Smirnova, and R. Bleck, 2004: Mesoscale weather prediction with the RUC Hybrid Isentropic-Terrain-Following Coordinate model. Mon. Wea. Rev., 132, 473–494.

Brooks, H. E., C. A. Doswell III, and J. Cooper, 1994: On the environments of tornadic and nontornadic mesocyclones. Wea. Forecasting, 9, 606–618.

Darkow, G. L., 1969: An analysis of over sixty tornado proximity soundings. Preprints, Sixth Conf. on Severe Local Storms, Amer. Meteor. Soc., Chicago, IL, 218-221.

Edwards, R., and R. L. Thompson, 2000: RUC-2 supercell proximity soundings, Part II: An independent assessment of supercell forecast parameters. Preprints, Twentieth Conf. on Severe Local Storms, Amer. Meteor. Soc., Orlando, FL, pp. 435–438.

Graves, C., and J. Moore, 2002: SLUBREW user's manual. Tech. rep., Saint Louis University, 3507 Laclede Ave, St. Louis, MO 63103.

Houze, Jr., R. A., B. F. Smull, and P. Dodge, 1990: Mesoscale organization of springtime rainstorms in Oklahoma. Mon. Wea. Rev., 118, 613–654.

Junker, N. W., 2001: Quantitative precipitation forecasting overview. URL http://meted.ucar.edu/qpf/qpfintro/index1.htm

Kelsch, M., 2002: COMET flash flood cases: Summary of characteristics. Preprints, Sixteenth Conf. on Hydrology, Amer. Meteor. Soc.

Koch, S., M. Desjardins, and P. Kocin, 1983: An interactive Barnes objective map analysis scheme to use with satellite and conventional data. J. Appl. Meteor., 17, 723–738.

Maddox, R. A., C. F. Chappell, and L. R. Hoxit, 1979: Synoptic and meso-α scale aspects of flash flood events. Bull. Amer. Meteor. Soc., 60, 115–123.

NCDC: National Climatic Data Center. COOP and NEXRAD Level II and Level III Digital Data, http://ncdc.noaa.gov

NOAA, 2006: Flash floods and floods - the awesome power! National Oceanic & Atmospheric Administration (NOAA),U.S. Dept. of Commerce, URL http://www.noaawatch.gov/floods.php http://www.weather.gov/floodsafety/

Rasmussen, E. N., and D. O. Blanchard, 1998: A baseline climatology of sounding-derived supercell and tornado forecast parameters. Wea. Forecasting, 13, 1148–1164.

Thompson, R. L., and R. Edwards, 2000: A comparison of Rapid Update Cycle (RUC-2) model soundings with observed soundings in supercell environments. Preprints, Twentieth Conf. on Severe Local Storms, Amer. Meteor. Soc., Orlando, FL.

_____, R. Edwards, J. A. Hart, K. L. Elmore, and P. Markowski, 2003: Close proximity soundings within supercell environments obtained from the Rapid Update Cycle. Wea. Forecasting, 18, 1243–1261.

UCAR: University Corporation for Atmospheric Research. Image Archive, URL http://locust.mmm.ucar.edu/case-selection/

USWRP, 2001: National need, vision, and interagency plan for FY 2000-2006: An implementation plan - qualitative precipitation forecast and data assimilation. URL http://www.esrl.noaa.gov/research/uswrp/

Weisman, M. L., M. S. Gilmore, and L. J. Wicker, 1998: The impact of convective storms on their local environment: What is an appropriate ambient sounding? Preprints, Nineteenth Conf. on Severe Local Storms, Amer. Meteor. Soc., Minneapolis, MN, pp. 238–241.

Wilks, D., 2006; Statistical Methods in the Atmospheric Sciences, Vol. 2. Academic Press, 627 pp.

WIST, 2002: Weather Information for Surface Transportation National Needs Assessment Report. Tech. Rep. FCM-R18-2002, Office of the Federal Coordinator for Meteorological Services and Supporting Research, U.S. Department of Commerce/NOAA.

____, 2005: Weather Information for Surface Transportation National Needs Assessment Report WIST Initiative Document. Tech. rep., Office of the Federal Coordinator for Meteorological Services and Supporting Research, U.S. Department of Commerce/NOAA.

6. TABLES

Table 1. Mean, median, and standard deviation associated with the sounding parameters for the four-inch synoptic-type rainfall events. These values are associated with the test cases (2006-2007).

Parameter	Mean	Median	Std Dev.
0-2 km Bulk Directional Shear	250	332	157
0-2 km Bulk Speed Shear	21	21	8
0-3 km Bulk Directional Shear	142	85	177
0-3 km Bulk Speed Shear	23	21	9
0-6 km Bulk Directional Shear	155	94	181
0-6 km Bulk Speed Shear	29	26	12
3-6 km Bulk Directional Shear	255	236	49
3-6 km Bulk Speed Shear	8	6	6
K Index	23	23	3
Precipitable Water	1.16	1.14	0.39
Subcloud Layer Relative Humidity	65	63	9
Surface-500 hPa Relative Humidity	53	54	14
Surface-500 hPa Theta-e	326	327	7
Convective Temperature	81	83	8
700-500 hPa Lapse Rates	19	20	2
850-500 hPa Convective Instability	-7	-7	6
CAPE	2648	2685	1259
CIN	126	119	139
Lid Strength Index	2	2	1
LCP	827	829	20
LFC	804	831	64
Distance between LFC-EL	612	621	69
Equilibrium Temperature	-64	-64	2
Warm Cloud Depth	3519	3883	983

Table 2. Same as Table 1, except for frontal-type rainfall events.

Parameter	Mean	Median	Std Dev.
0-2 km Bulk Directional Shear	331	331	17
0-2 km Bulk Speed Shear	26	26	11
0-3 km Bulk Directional Shear	344	344	19
0-3 km Bulk Speed Shear	27	27	13
0-6 km Bulk Directional Shear	188	188	235
0-6 km Bulk Speed Shear	27	27	15
3-6 km Bulk Directional Shear	272	272	30
3-6 km Bulk Speed Shear	11	11	6
K Index	35	35	4
Precipitable Water	1.73	1.71	0.30
Subcloud Layer Relative Humidity	74	75	9
Surface-500 hPa Relative Humidity	72	70	11
Surface-500 hPa Theta-e	336	336	6
Convective Temperature	87	85	6
700-500 hPa Lapse Rates	18	18	4
850-500 hPa Convective Instability	-9	-9	5
CAPE	2897	2583	1396
CIN	122	114	103
Lid Strength Index	1	1	1
LCP	834	833	35
LFC	783	769	62
Distance between LFC-EL	639	623	65
Equilibrium Temperature	-70	-70	3
Warm Cloud Depth	4041	4079	506

Table 3. Same as Table 1, except for the two-inch synoptic-type rainfall events.

Parameter	Mean	Median	Std Dev.
0-2 km Bulk Directional Shear	349	349	6
0-2 km Bulk Speed Shear	28	28	0.1
0-3 km Bulk Directional Shear	175	175	246
0-3 km Bulk Speed Shear	28	28	2
0-6 km Bulk Directional Shear	13	13	9
0-6 km Bulk Speed Shear	22	22	1
3-6 km Bulk Directional Shear	307	307	4
3-6 km Bulk Speed Shear	10	10	2
K Index	37	37	2
Precipitable Water	1.42	1.42	0.27
Subcloud Layer RH	57	57	2
Sfc-500 hPa RH	49	49	8
Sfc-500 hPa Theta-e	334	334	2
Convective Temperature	96	96	3
700-500 hPa Lapse Rates	17	17	1
850-500 hPa Convective Instability	-13	-13	4
CAPE	1889	1889	1118
CIN	148	148	179
Lid Strength Index	4	4	1
LCP	769	769	53
LFC	728	728	21
Distance between LFC-EL	558	558	41
Equilibrium Temperature	-60	-60	3
Warm Cloud Depth	3319	3319	1219

Table 4. Same as Table 1, except for the two-inch frontal-type rainfall events.

Parameter	Mean	Median	Std Dev.
0-2 km Bulk Directional Shear	15	14	6
0-2 km Bulk Speed Shear	16	16	3
0-3 km Bulk Directional Shear	24	24	5
0-3 km Bulk Speed Shear	18	18	2
0-6 km Bulk Directional Shear	38	36	5
0-6 km Bulk Speed Shear	18	18	5
3-6 km Bulk Directional Shear	309	324	43
3-6 km Bulk Speed Shear	6	5	2
K Index	29	29	5
Precipitable Water	1.17	1.16	0.25
Subcloud Layer Relative Humidity	66	63	9
Surface-500 hPa Relative Humidity	51	45	17
Surface-500 hPa Theta-e	328	327	7
Convective Temperature	82	84	10
700-500 hPa Lapse Rates	19	20	3
850-500 hPa Convective Instability	-13	-12	10
CAPE	2437	2504	1639
CIN	72	28	94
Lid Strength Index	2	3	2
LCP	828	823	70
LFC	761	735	120
Distance between LFC-EL	546	561	138
Equilibrium Temperature	-62	-62	2
Warm Cloud Depth	3217	3440	1558

Table 5. Mean, median, and standard deviation associated with the sounding parameters for the four-inch synoptic type rainfall events. These values are associated with the three-year (2003-2005), original dataset.

Parameter	Mean	Median	Std Dev.
0-2 km Bulk Directional Shear	183	249	142
0-2 km Bulk Speed Shear	25	24	16
0-3 km Bulk Directional Shear	175	230	135
0-3 km Bulk Speed Shear	24	21	15
0-6 km Bulk Directional Shear	179	154	126
0-6 km Bulk Speed Shear	21	14	14
3-6 km Bulk Directional Shear	286	303	61
3-6 km Bulk Speed Shear	9	8	4
K Index	31	32	8
Precipitable Water	1.48	1.45	0.38
Subcloud Layer Relative Humidity	75	79	13
Surface-500 hPa Relative Humidity	61	60	11
Surface-500 hPa Theta-e	332	333	9
Convective Temperature	86	87	10
700-500 hPa Lapse Rates	18	17	2
850-500 hPa Convective Instability	-12	-12	10
CAPE	3526	3173	2063
CIN	183	92	251
Lid Strength Index	2	2	2
LCP	832	842	48
LFC	774	798	86
Distance between LFC-EL	591	625	140
Equilibrium Temperature	-58	-62	12
Warm Cloud Depth	4039	4417	1252

Table 6. Same as Table 5, except for the frontal-type rainfall events.

Parameter	Mean	Median	Std Dev.
0-2 km Bulk Directional Shear	265	297	102
0-2 km Bulk Speed Shear	21	19	12
0-3 km Bulk Directional Shear	237	301	129
0-3 km Bulk Speed Shear	19	17	11
0-6 km Bulk Directional Shear	195	263	137
0-6 km Bulk Speed Shear	16	14	8
3-6 km Bulk Directional Shear	274	278	65
3-6 km Bulk Speed Shear	10	10	4
K Index	31	32	10
Precipitable Water	1.38	1.45	0.37
Subcloud Layer Relative Humidity	68	68	15
Surface-500 hPa Relative Humidity	61	65	15
Surface-500 hPa Theta-e	330	331	9
Convective Temperature	87	87	11
700-500 hPa Lapse Rates	18	18	2
850-500 hPa Convective Instability	-10	-11	11
CAPE	2909	2920	1965
CIN	164	56	256
Lid Strength Index	4	3	2
LCP	810	819	60
LFC	748	750	85
Distance between LFC-EL	547	602	164
Equilibrium Temperature	-56	-59	15
Warm Cloud Depth	3389	3812	1475

Table 7. Same as Table 5, except for the two-inch synoptic-type rainfall events.

Parameter	Mean	Median	Std Dev.
0-2 km Bulk Directional Shear	223	302	137
0-2 km Bulk Speed Shear	28	25	15
0-3 km Bulk Directional Shear	201	287	140
0-3 km Bulk Speed Shear	25	25	13
0-6 km Bulk Directional Shear	177	125	130
0-6 km Bulk Speed Shear	22	21	10
3-6 km Bulk Directional Shear	295	300	24
3-6 km Bulk Speed Shear	12	12	5
K Index	22	24	11
Precipitable Water	1.04	1.02	0.39
Subcloud Layer Relative Humidity	64	67	16
Surface-500 hPa Relative Humidity	53	52	14
Surface-500 hPa Theta-e	323	322	9
Convective Temperature	84	84	11
700-500 hPa Lapse Rates	19	19	2
850-500 hPa Convective Instability	-4	-4	11
CAPE	2010	1547	1900
CIN	300	136	427
Lid Strength Index	4	3	2
LCP	802	812	63
LFC	737	731	99
Distance between LFC-EL	506	526	151
Equilibrium Temperature	-53	-57	15
Warm Cloud Depth	2986	3149	1275

Table 8. Same as Table 5, except for the two-inch frontal-type rainfall events.

Parameter	Mean	Median	Std Dev.
0-2 km Bulk Directional Shear	238	286	118
0-2 km Bulk Speed Shear	21	20	11
0-3 km Bulk Directional Shear	222	278	128
0-3 km Bulk Speed Shear	19	19	10
0-6 km Bulk Directional Shear	197	221	122
0-6 km Bulk Speed Shear	15	14	9
3-6 km Bulk Directional Shear	279	295	78
3-6 km Bulk Speed Shear	9	10	3
K Index	29	31	8
Precipitable Water	1.32	1.32	0.26
Subcloud Layer Relative Humidity	63	65	13
Surface-500 hPa Relative Humidity	53	53	9
Surface-500 hPa Theta-e	332	332	6
Convective Temperature	90	90	10
700-500 hPa Lapse Rates	20	20	2
850-500 hPa Convective Instability	-12	-14	8
CAPE	2979	2967	1534
CIN	230	120	260
Lid Strength Index	3	3	2
LCP	791	788	55
LFC	728	736	56
Distance between LFC-EL	550	551	66
Equilibrium Temperature	-58	-59	5
Warm Cloud Depth	3532	3396	874

7. ILLUSTRATIONS

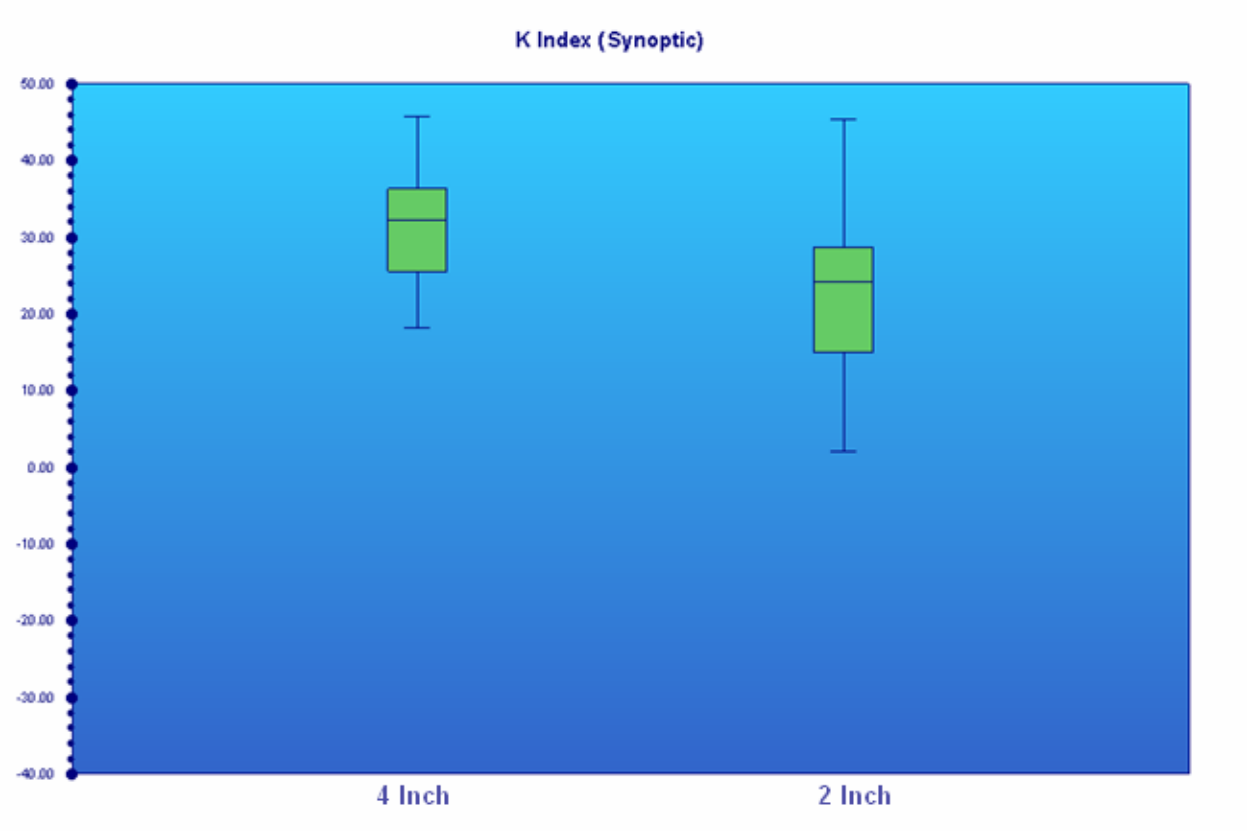

Figure 1. Boxplots of K index for four-inch (left) and two-inch (right) rainfall days associated with a synoptic-type rainfall setting. There is a noticeable difference in K index values from the two-inch to four-inch categories.

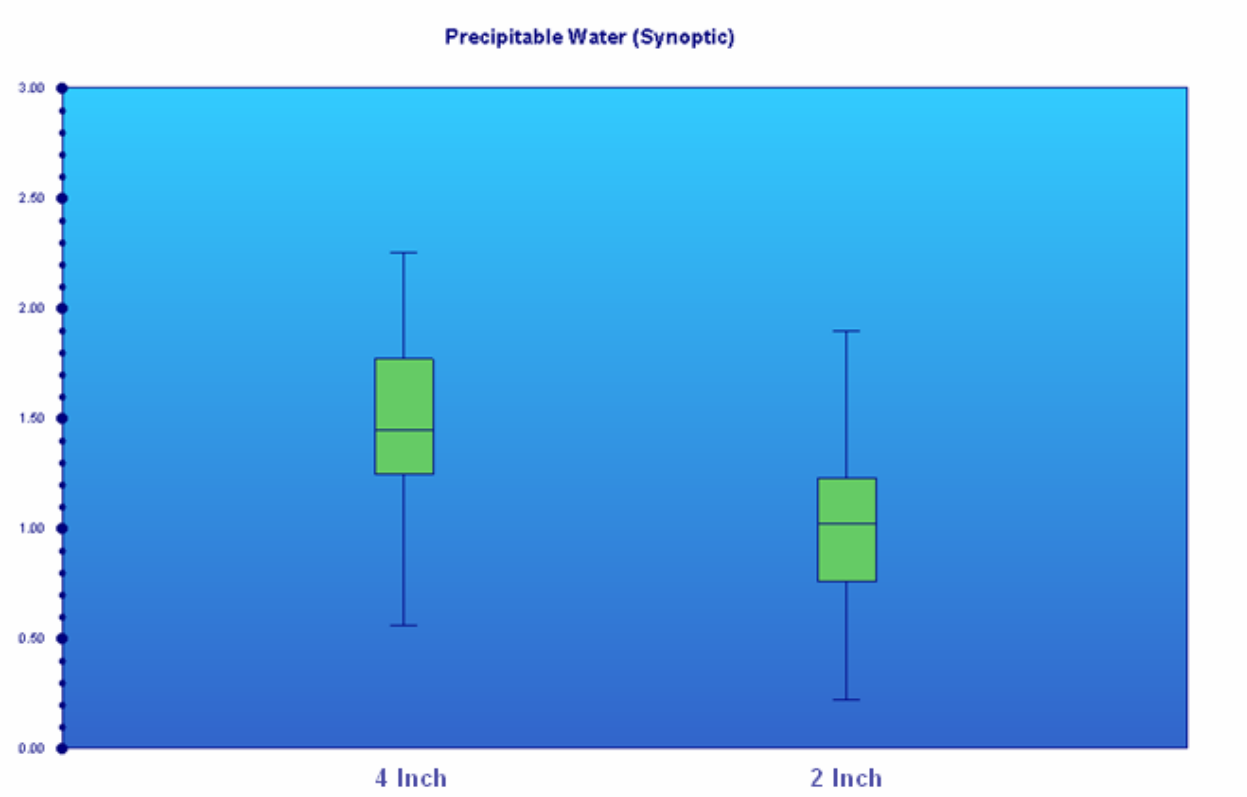

Figure 2. Same as Figure 1, except for PW (values in inches).

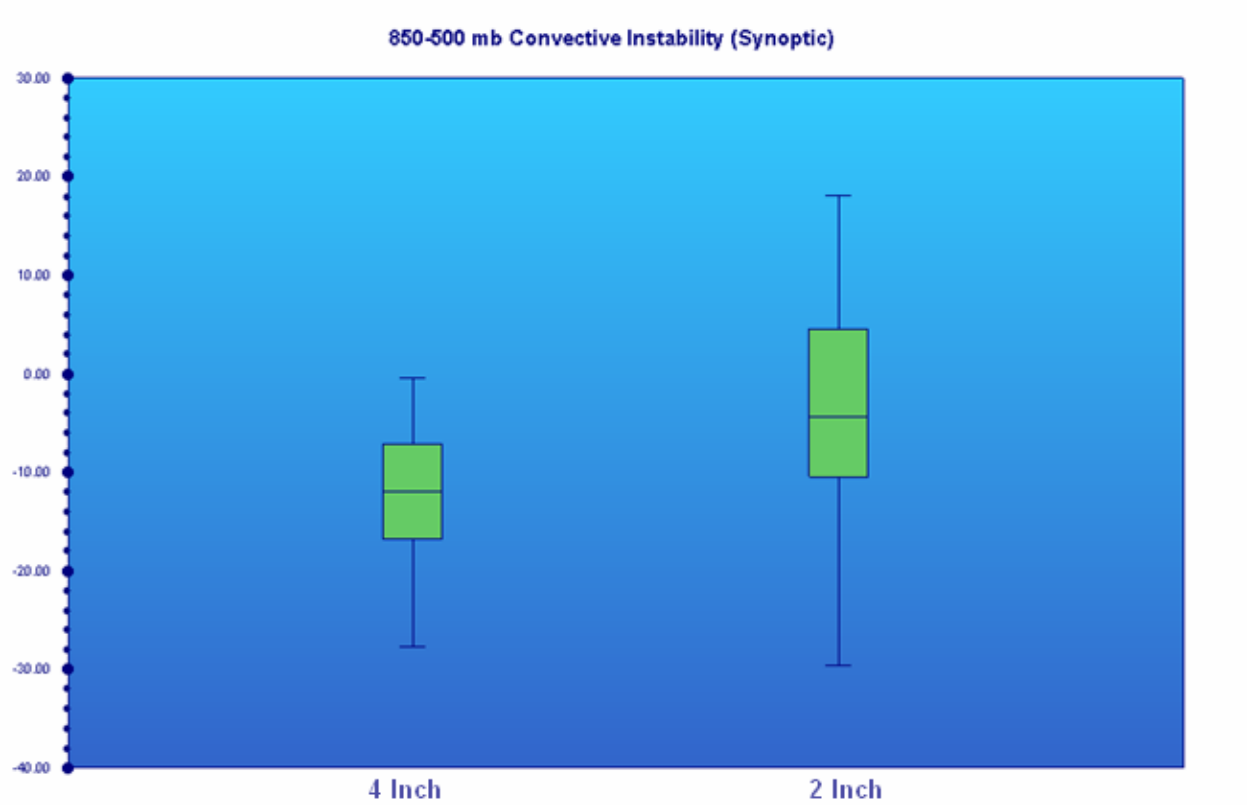

Figure 3. Same as Figure 1, except for 850-500 hPa Convective Instability (values in Kelvin).

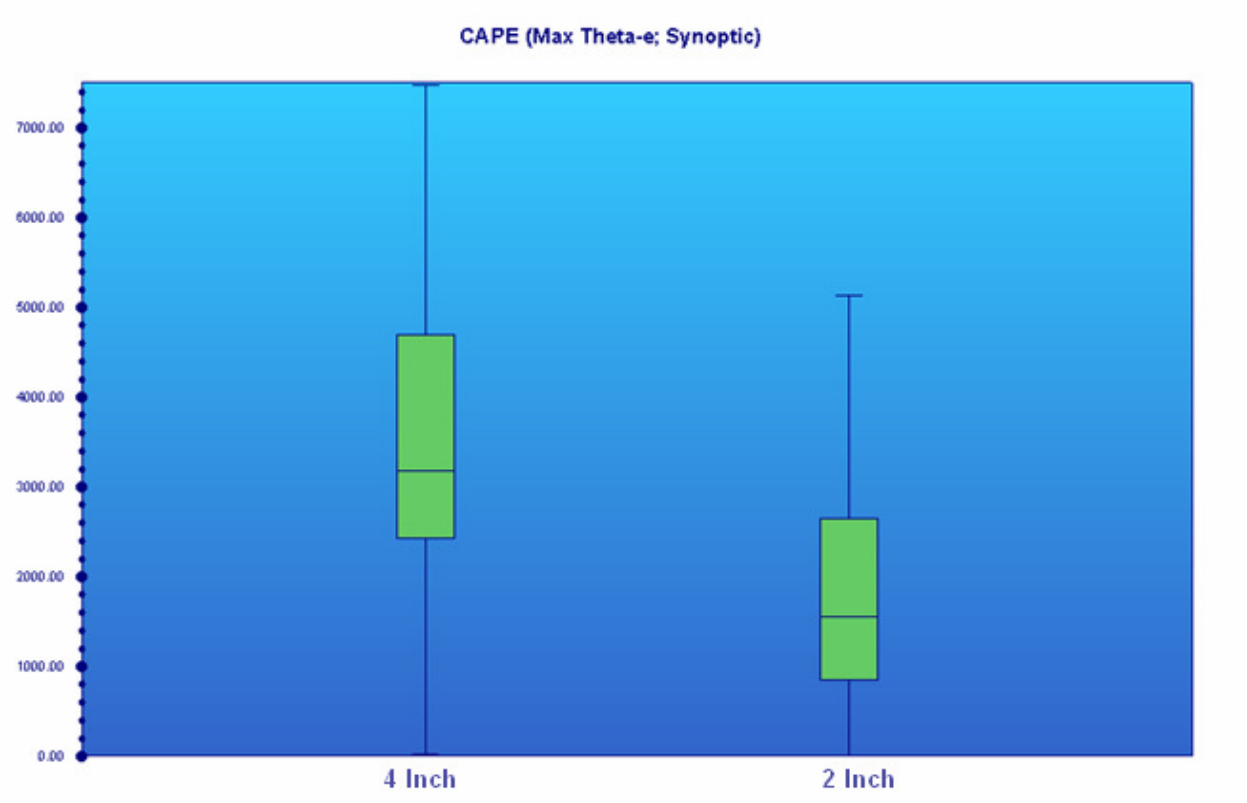

Figure 4. Same as Figure 1, except for the most unstable parcel CAPE (values in Jkg^{-1}).

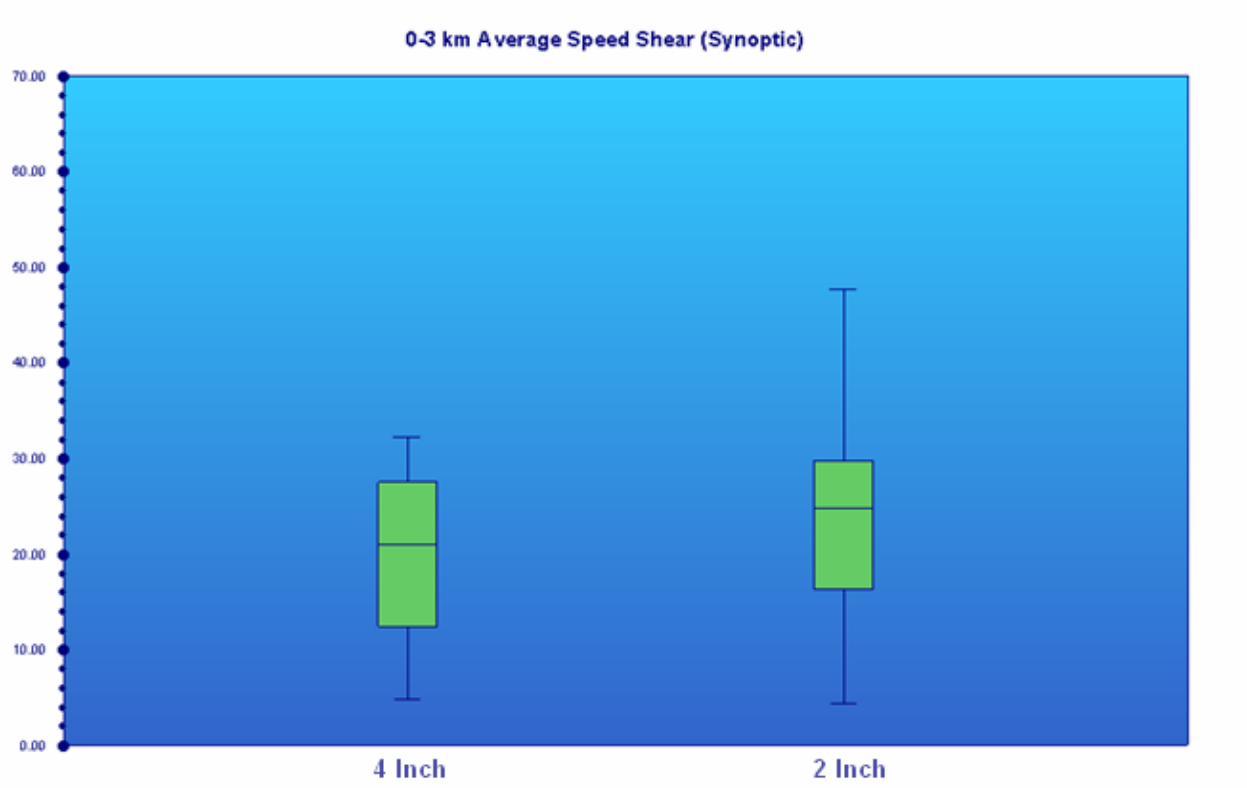

Figure 5. Same as Figure 1, except for 0-3 km Bulk Speed Shear (values in ms^{-1}).

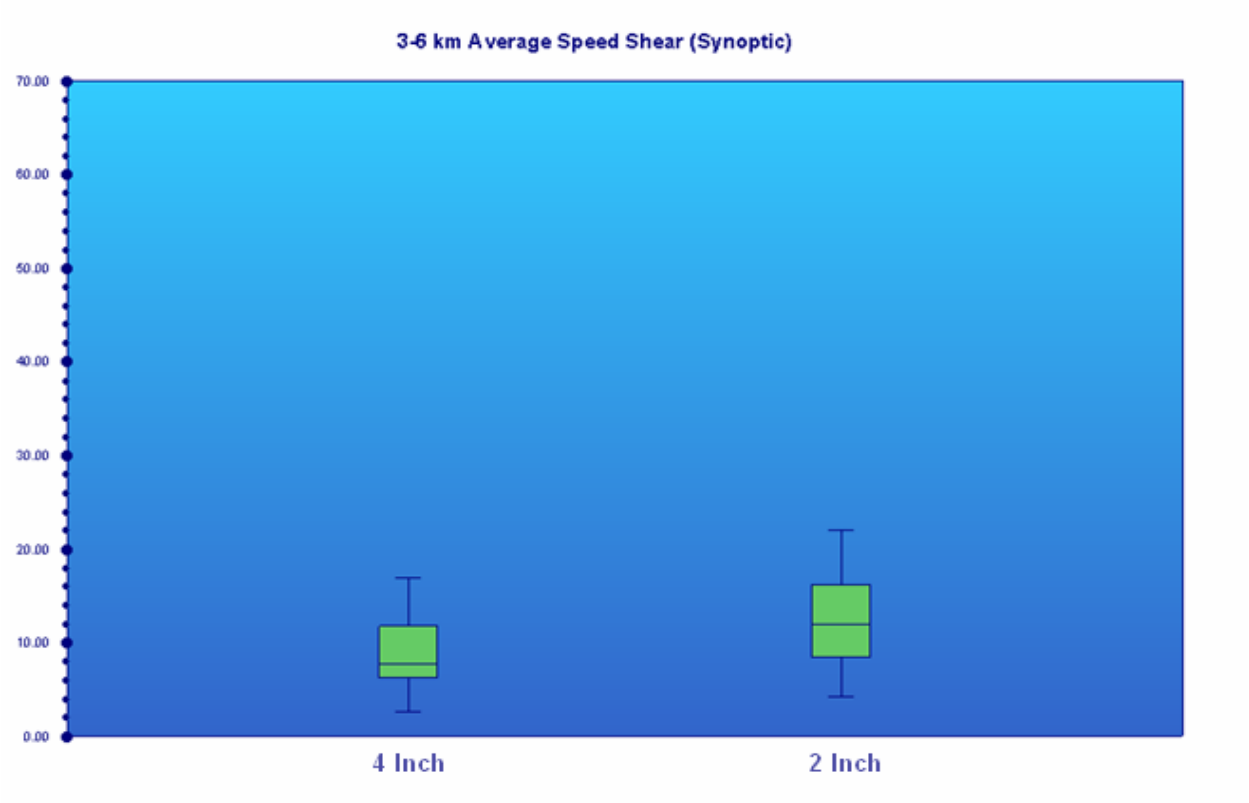

Figure 6. Same as Figure 1, except for 3-6 km Bulk Speed Shear (values in ms^{-1}).

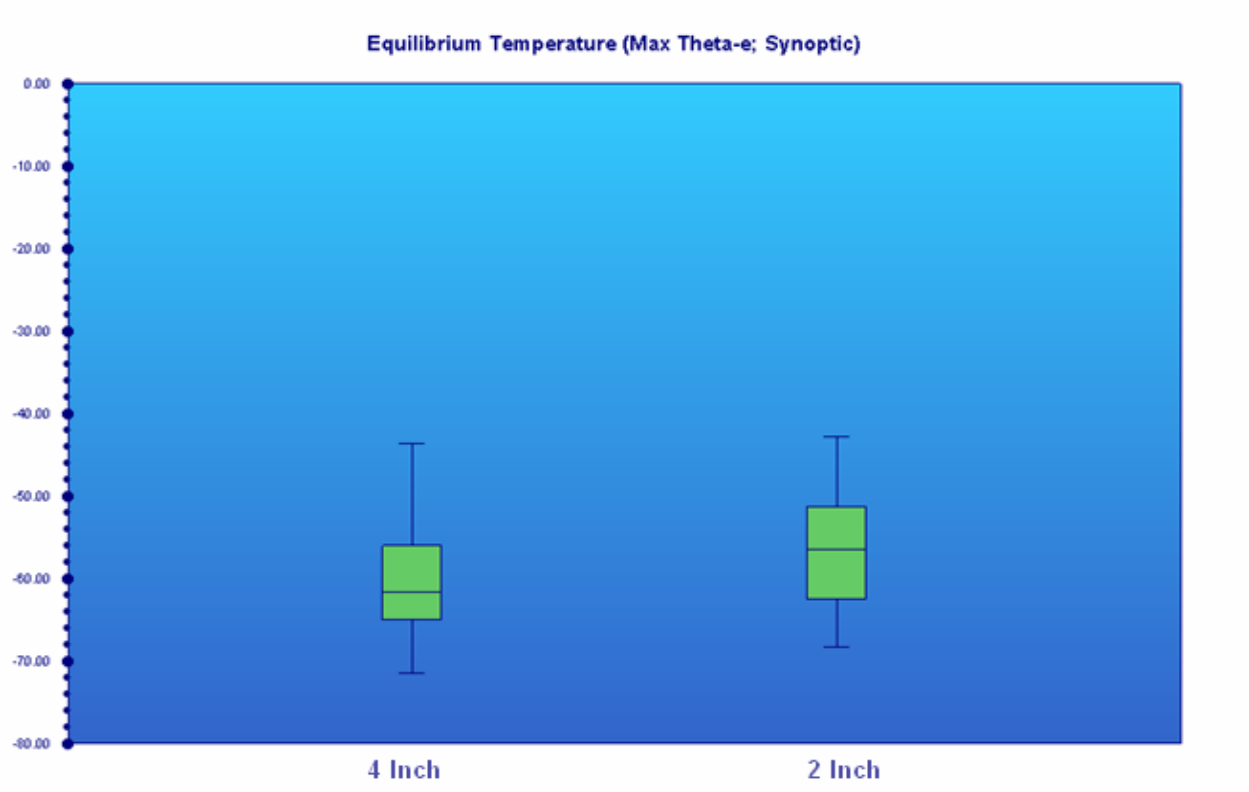

Figure 7. Same as Figure 1, except for Equilibrium Temperature using the most unstable parcel (values in ℃).

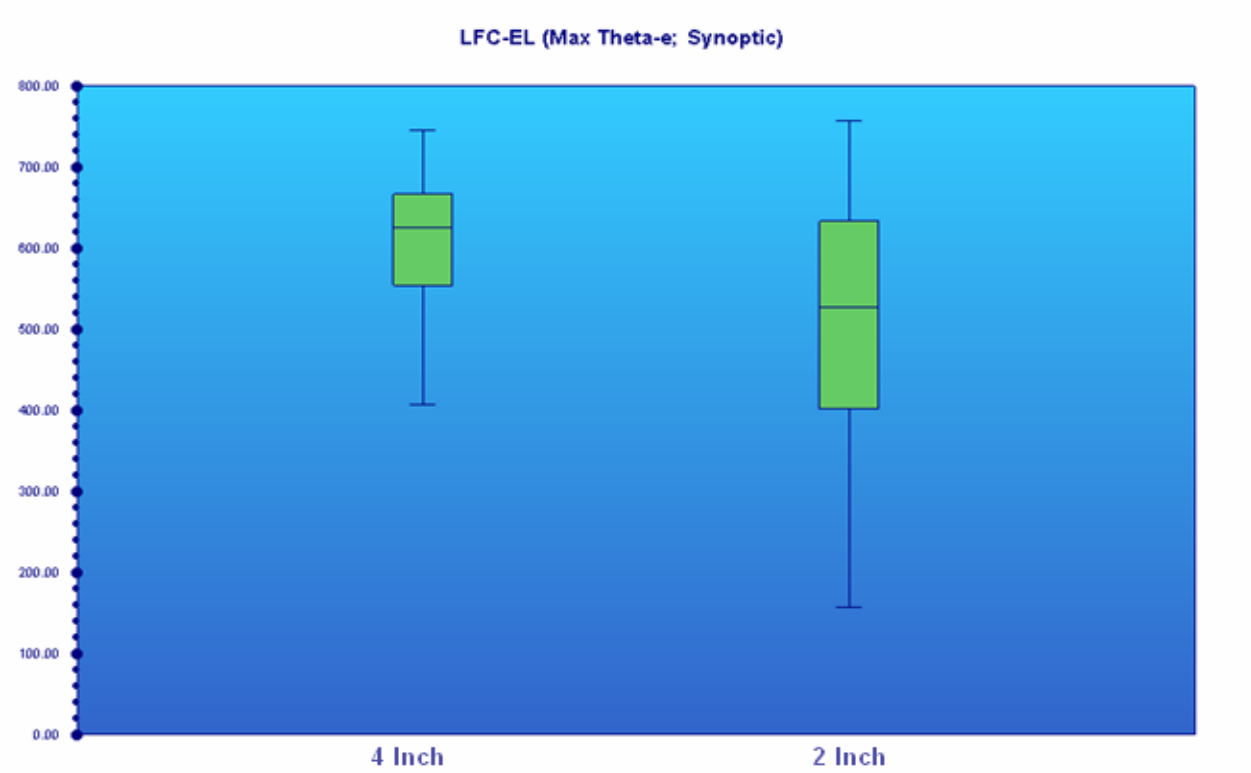

Figure 8. Same as Figure 1, except for the distance between the LFC to the EL using the most unstable parcel (values in hPa).

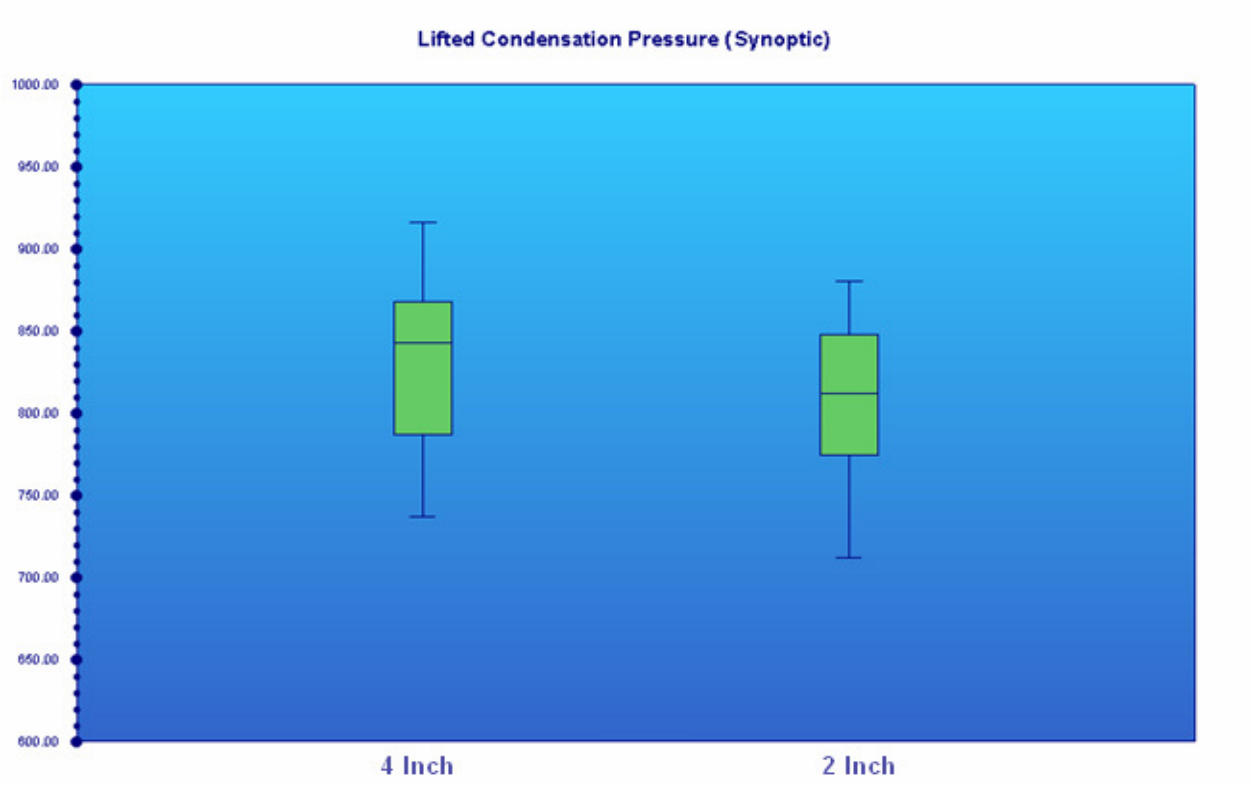

Figure 9. Same as Figure 1, except for LCP (values in hPa).

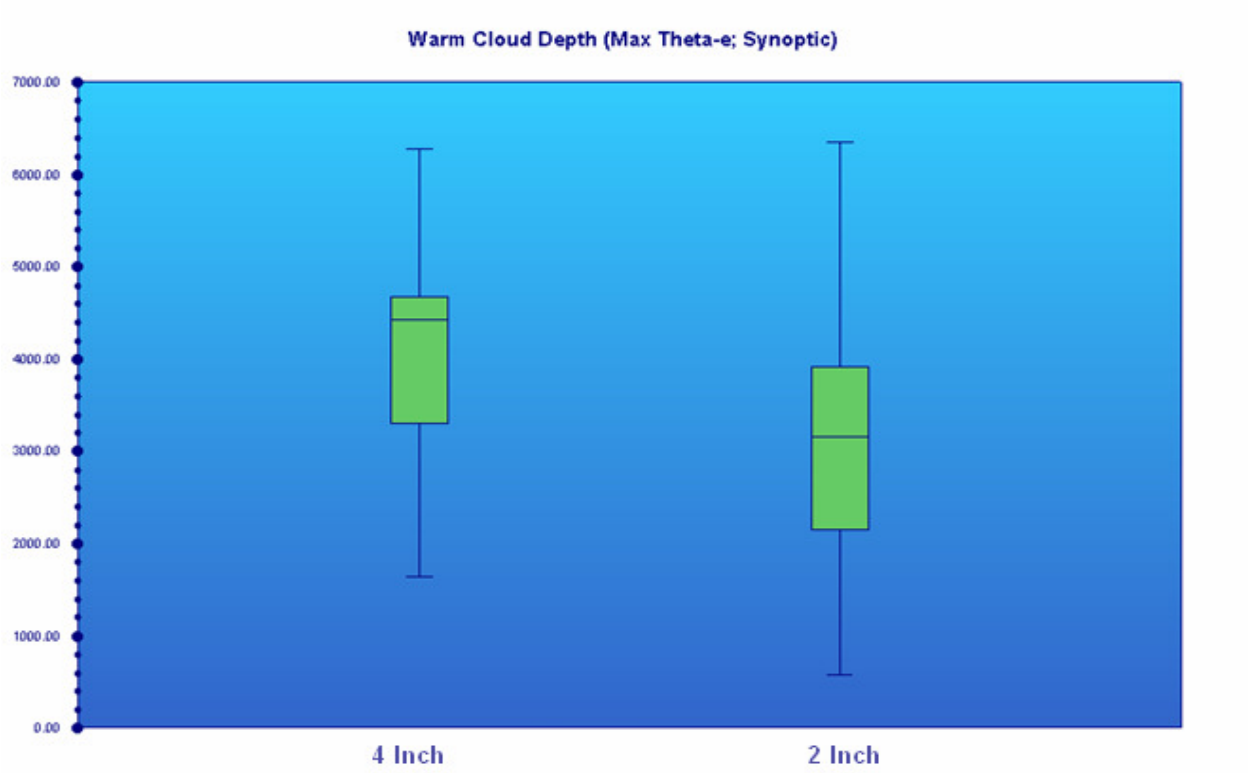

Figure 10. Same as Figure 1, except for Warm Cloud Depth using the most unstable parcel (values in meters).

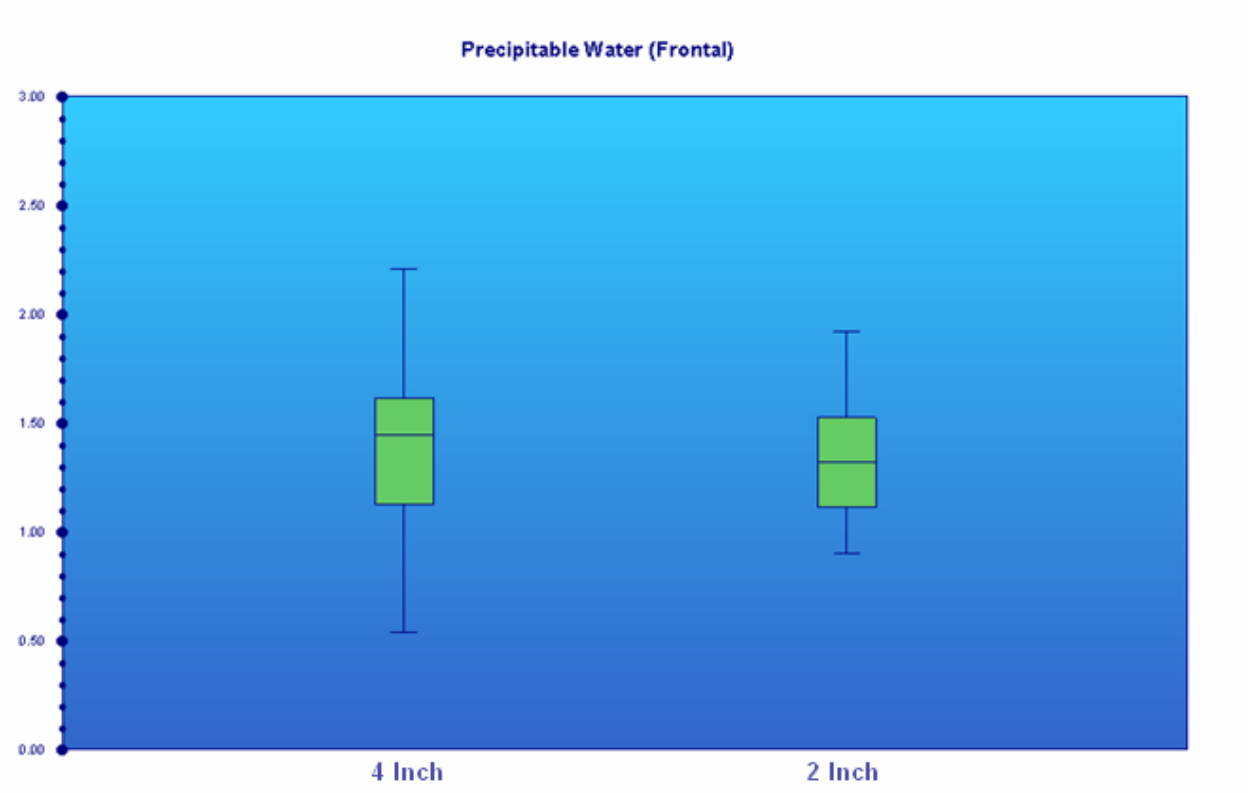

Figure 11. Boxplots of PW for four-inch (left) and two-inch (right) rainfall days associated with a frontal-type heavy rainfall setting (values in inches).

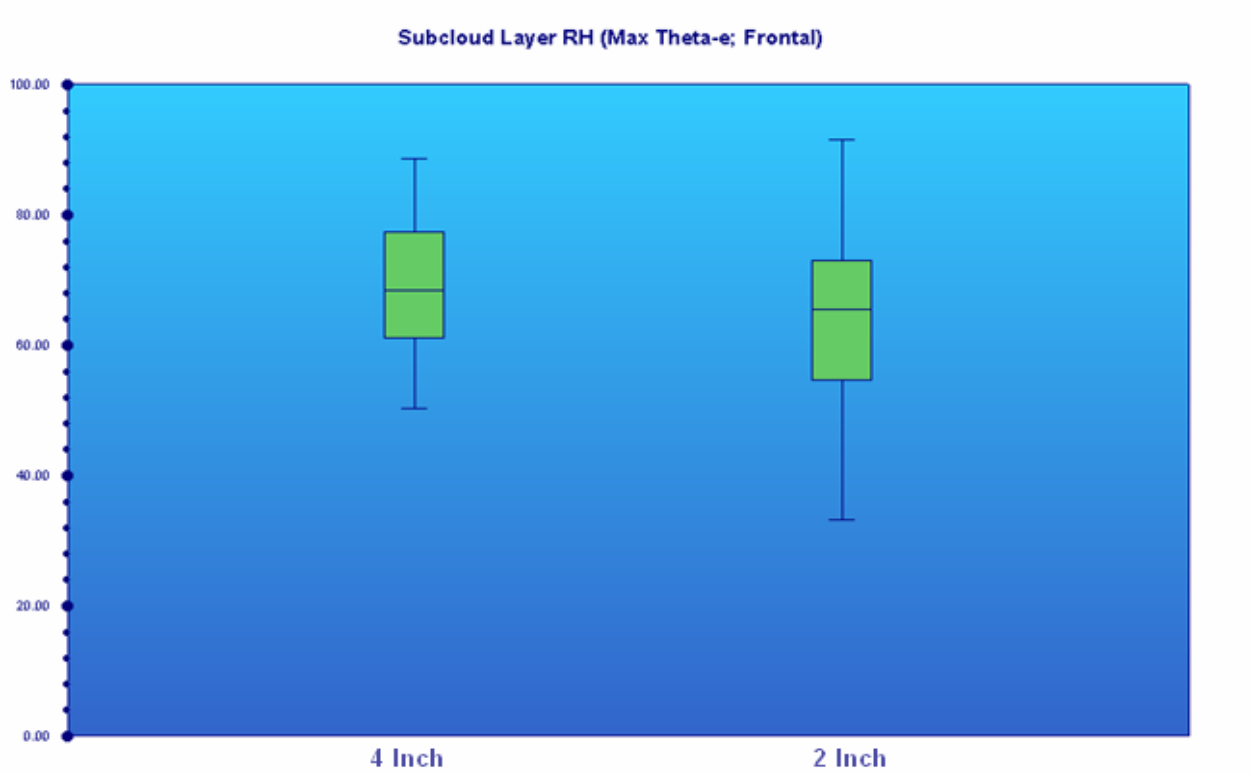

Figure 12. Same as Figure 11, except for Subcloud Layer Relative Humidity using the most unstable parcel (values in %).

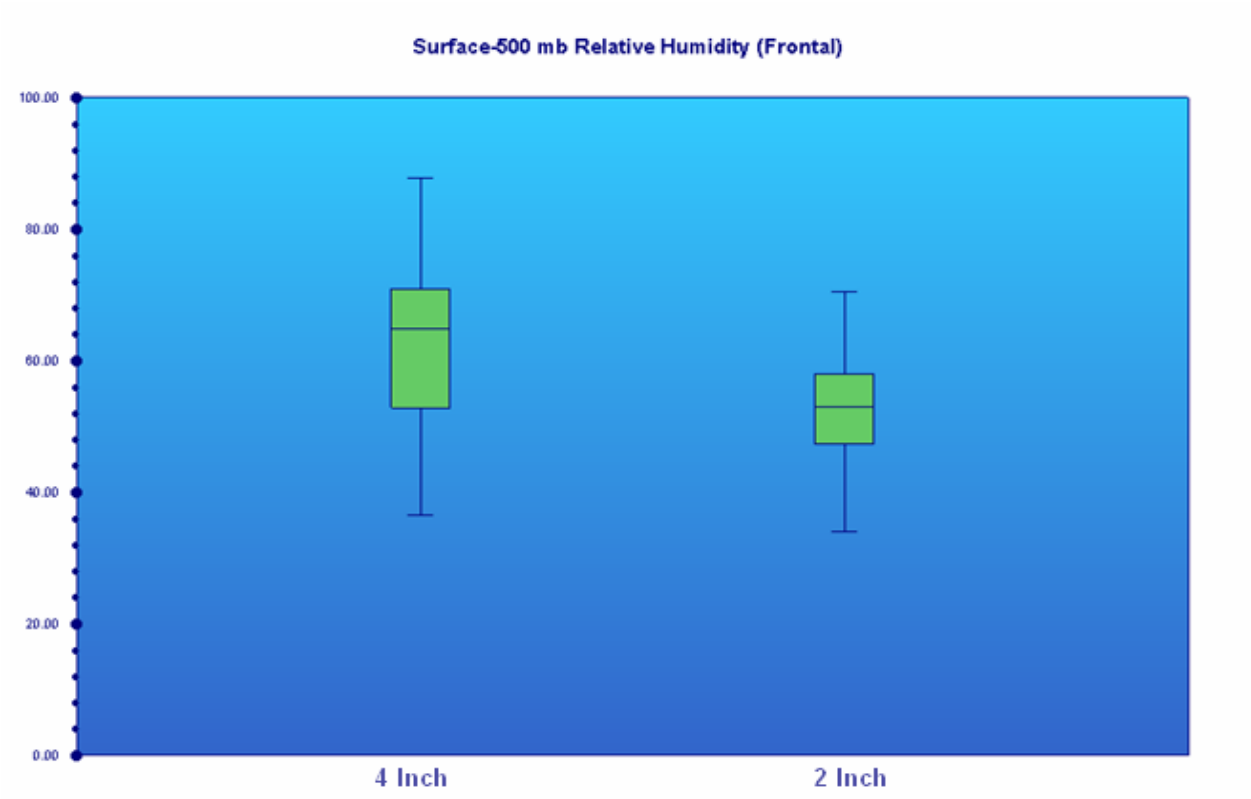

Figure 13. Same as Figure 11, except for Surface to 500 hPa Relative Humidity (values in %).

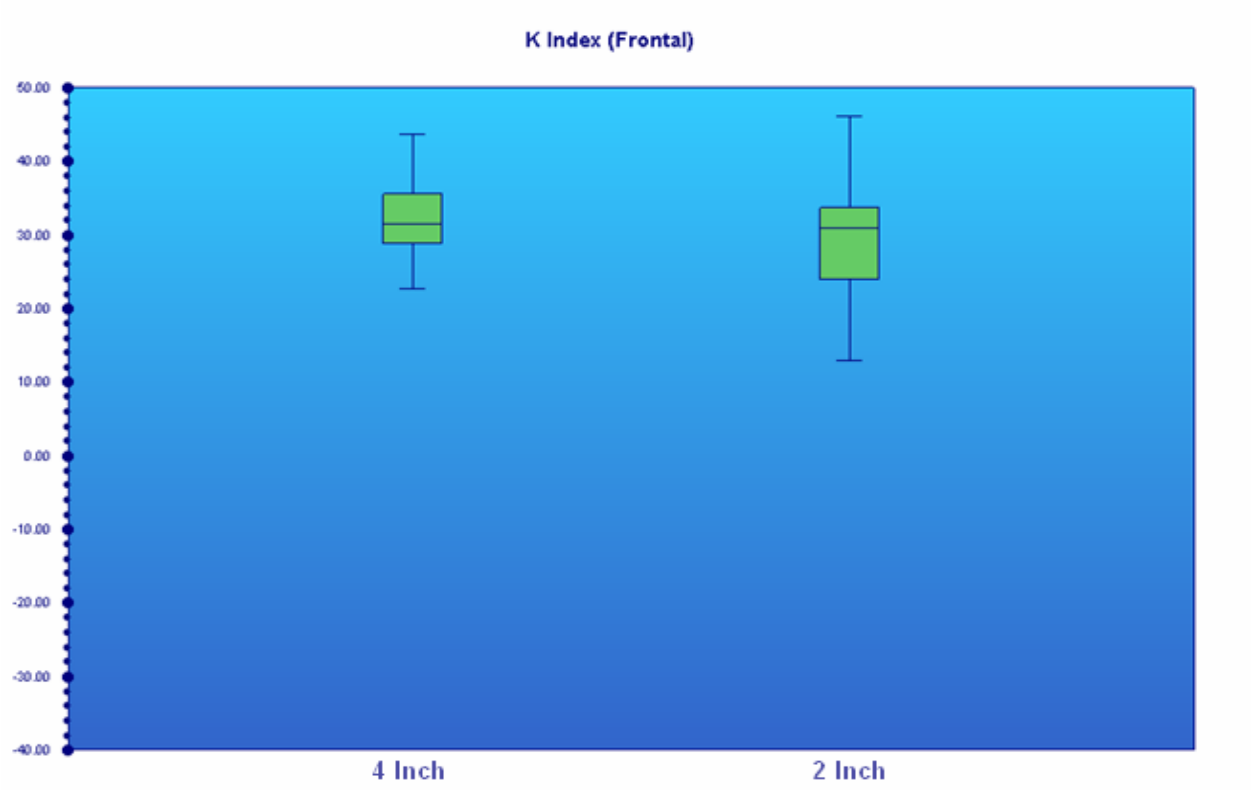

Figure 14. Same as Figure 11, except for K Index.

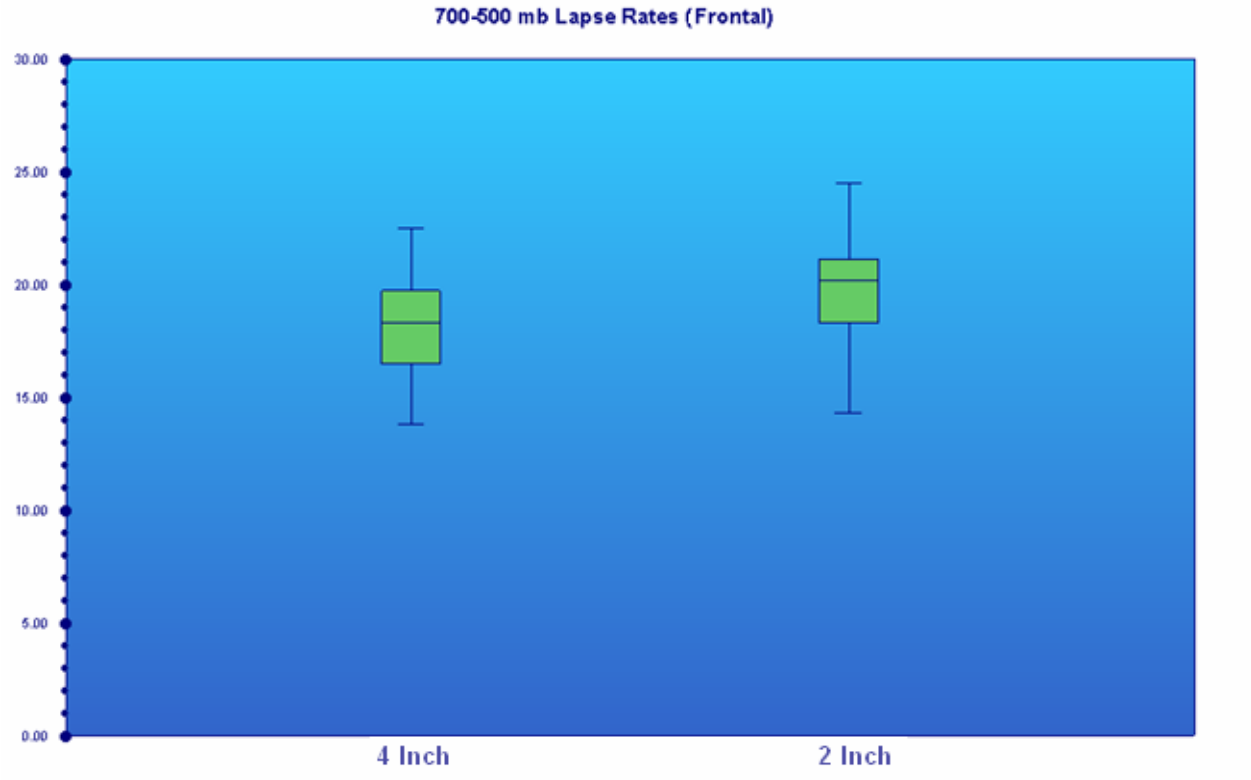

Figure 15. Same as Figure 11, except for 700 to 500 hPa Lapse Rates (values in ℃).

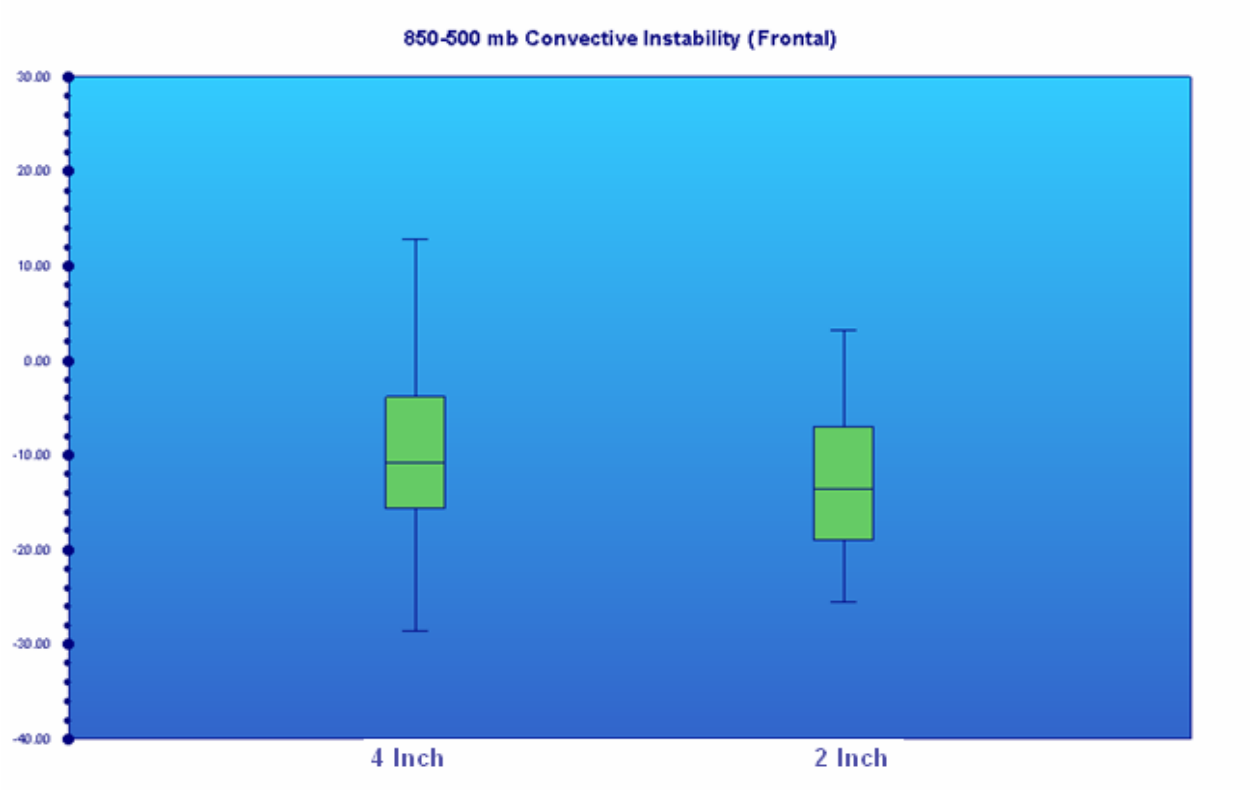

Figure 16. Same as Figure 11, except for 850 to 500 hPa Convective Instability (values in Kelvin).

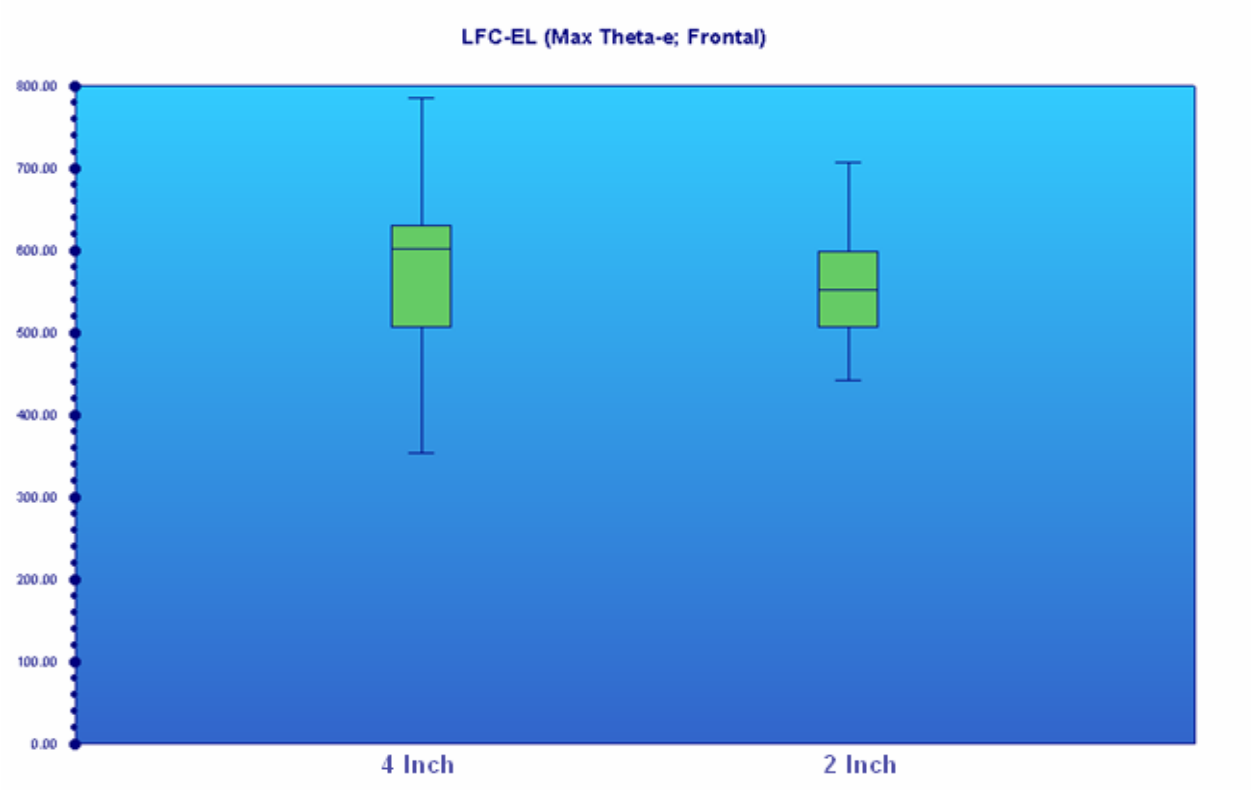

Figure 17. Same as Figure 11, except for the distance between the LFC to the EL using the most unstable parcel (values in hPa).

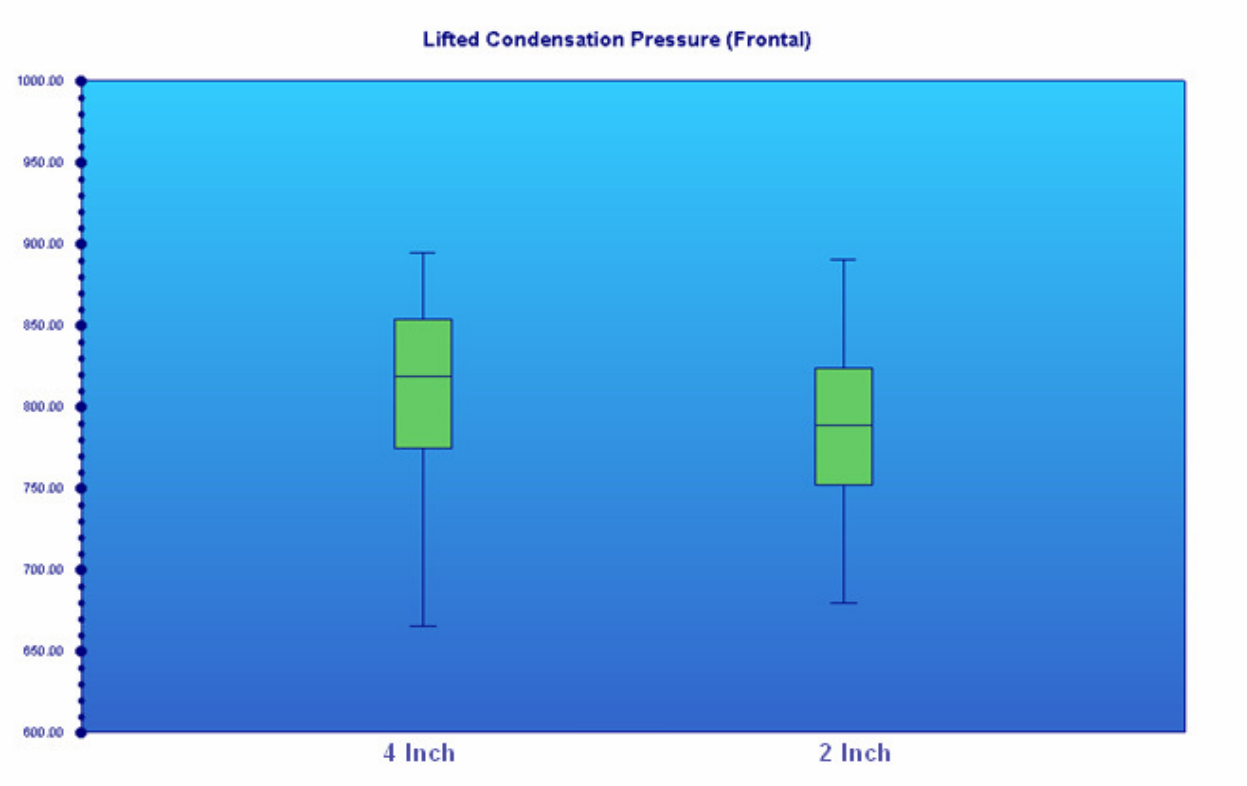

Figure 18. Same as Figure 11, except for the LCP (values in hPa).

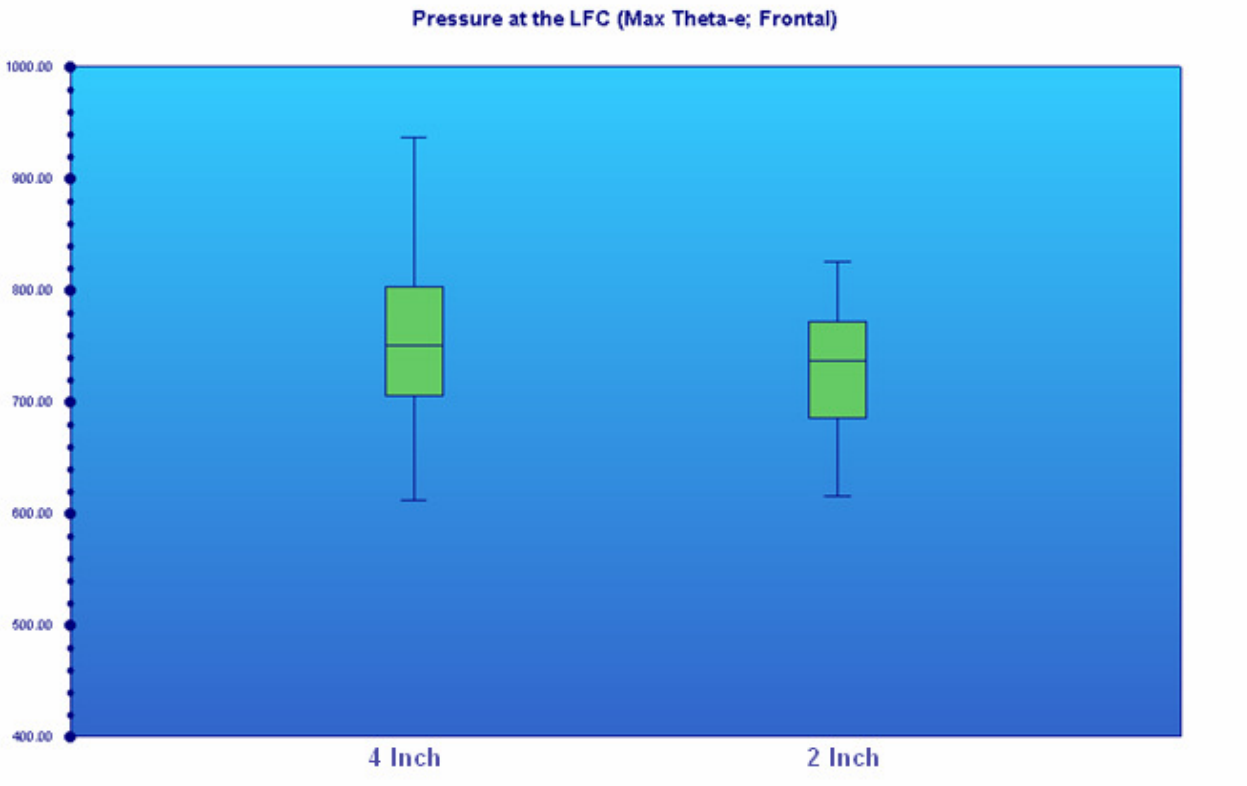

Figure 19. Same as Figure 11, except for the pressure at the LFC using the most unstable parcel (values in hPa).

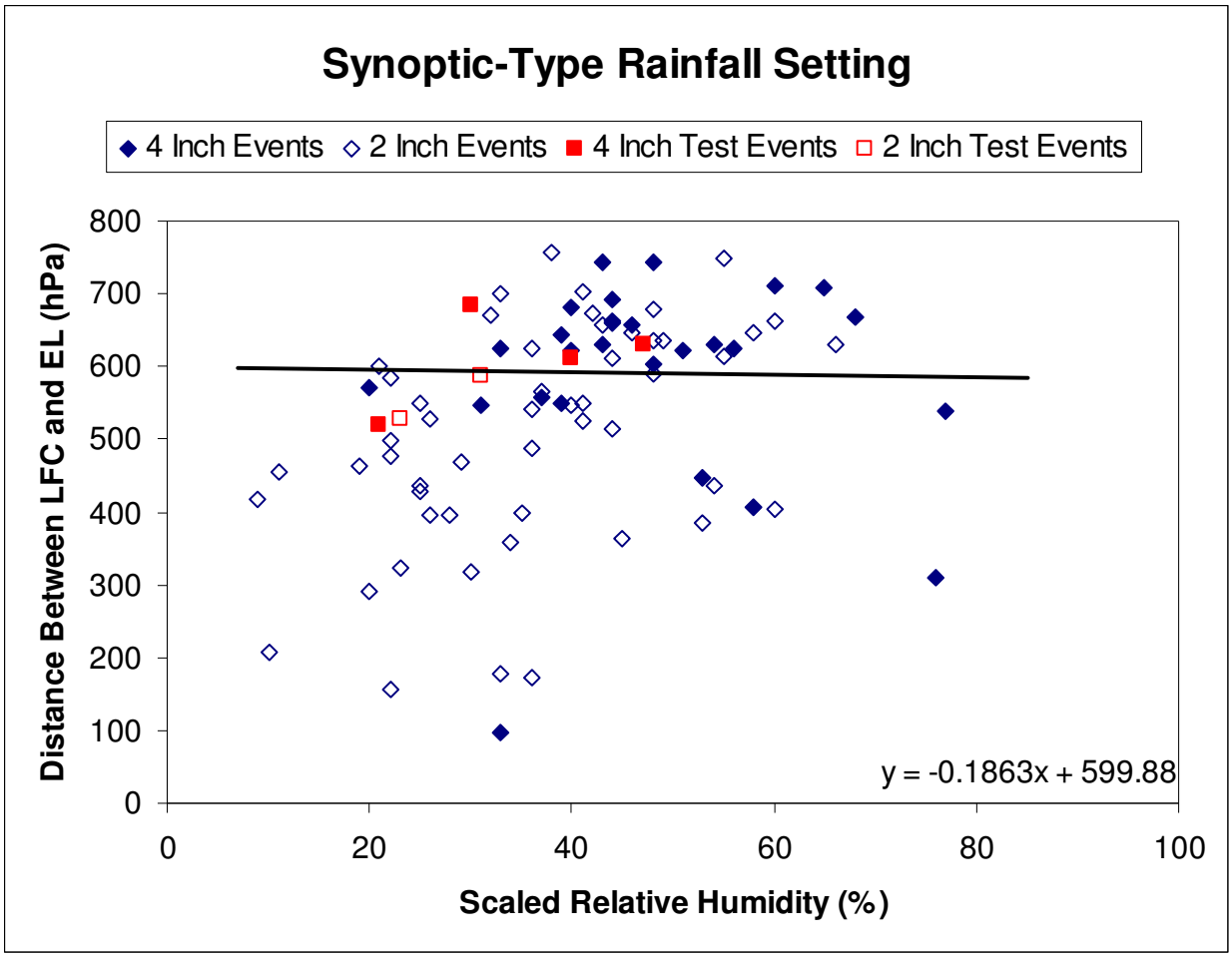

Figure 20. Scatterplot illustrating the spread associated with the scaled product of the subcloud layer relative humidity and surface to 500 hPa relative humidity plotted against the distance between the LFC and EL for four-inch and two-inch rainfall events. These events are associated with a synoptic-type setting. The filled and unfilled diamonds correspond to the four-inch and two-inch events, respectively, for the original, three-year dataset (2003-2005). The filled and unfilled squares correspond to the four-inch and two-inch events, respectively, for the test cases (2006-2007). The dark line best distinguishes the difference between four-inch and two-inch rainfall events with the equation given in the lower right hand corner. Events that fall above this line have a greater chance of being four-inch events, while events that fall below this line tend to have a greater chance of being two-inch events.

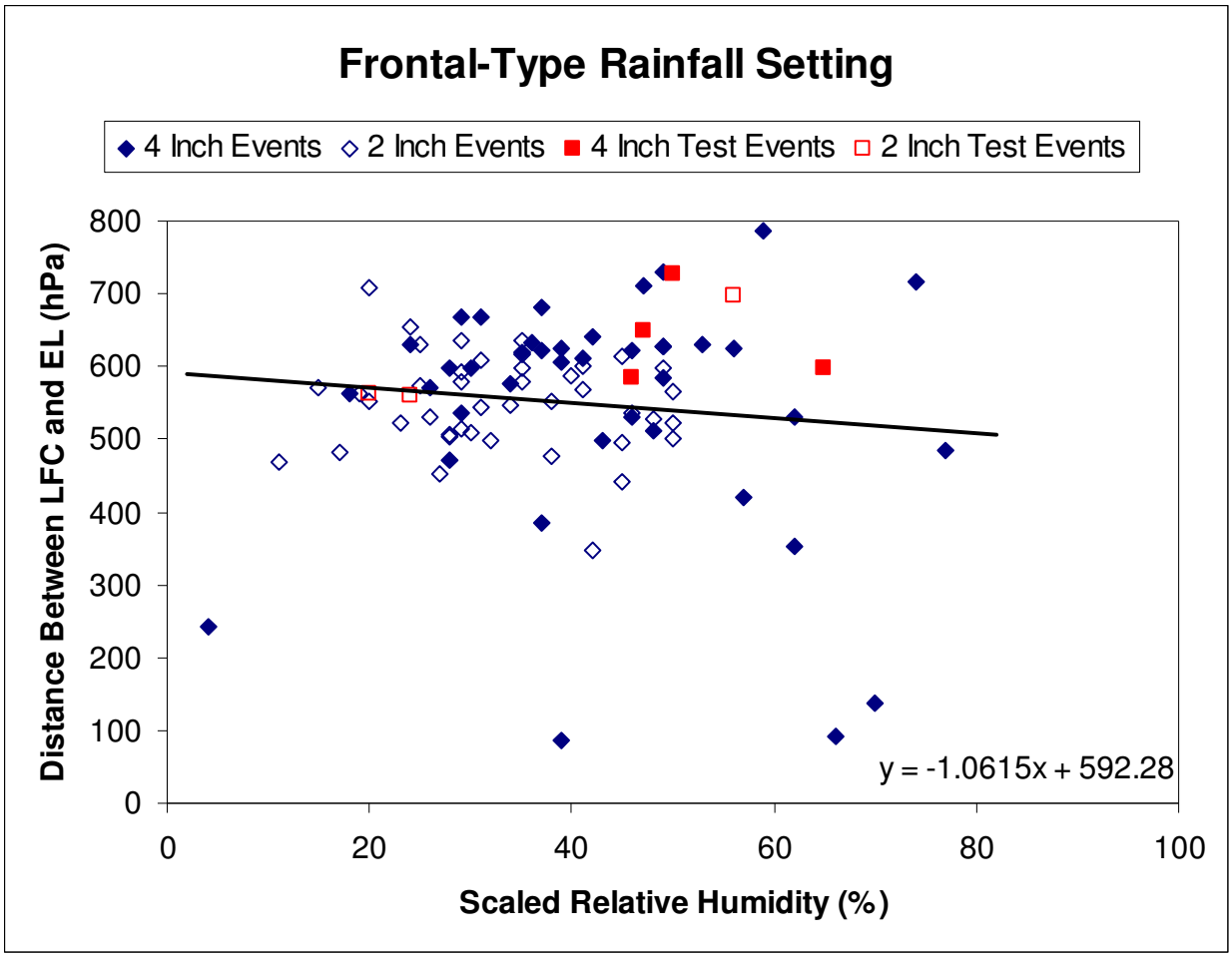

Figure 21. Same as Figure 20, except for frontal-type events.